Wideband Propagation Measurements at 30.3 GHz Through a Pecan Orchard in Texas

Peter B. Papazian*, David L. Jones** and Richard H. Espeland***

Wideband propagation measurements were made in a pecan orchard in Texas during April and August of 1990 to examine the propagation characteristics of millimeter-wave signals through vegetation. Measurements were made on tree obstructed paths with and without leaves.

The study presents narrowband attenuation data at 9.6 and 28.8 GHz as well as wideband impulse response measurements at 30.3 GHz. The wideband probe (Violette et al., 1983), provides amplitude and delay of reflected and scattered signals and bit-error rate. This is accomplished using a 500 MBit/sec pseudo-random code to BPSK modulate a 28.8 GHz carrier. The channel impulse response is then extracted by cross correlating the received pseudo-random sequence with a locally generated replica.

Key words: attenuation; delay spread; impulse response; millimeter-wave propagation; vegetation; wideband

I. INTRODUCTION

Over the past eight years, the Institute for Telecommunication Sciences (ITS) has conducted a variety of experiments in an effort to characterize the propagation of millimeter-wave signals through vegetation. These experiments involved the measurement of the received strength of narrowband millimeter-wave signals propagated through both coniferous and deciduous vegetation, at frequencies of 9.6, 28.8, 57.6 and 96.1 GHz. The results of these measurements have revealed much about the variation of received signal level with parameters such as carrier frequency, antenna polarization, antenna pointing angle, antenna position, foliage depth, and type of vegetation (Jones et al., 1989; Schwering et al., 1988; Violette et al., 1981; Violette et al., 1983).

As an extension of this work, ITS has configured its wideband millimeter-wave probe to make similar measurements. The wideband probe can provide a more complete characterization of the effects

---

* Peter Papazian is with the Institute for Telecommunication Sciences, National Telecommunications and Information Adminstration, U. S. Department of Commerce, Boulder, CO. 80303.

** David L. Jones is a former employee of the Institute for Telecommunication Sciences, National Telecommunications and Information Adminstration, U. S. Department of Commerce, Boulder, CO 80303.

*** Richard H. Espeland is an independent contractor.

of vegetation on the propagation of millimeter-wave signals. The wideband probe consists of a 30.3 GHz millimeter-wave carrier onto which a 500 Mb/s digital signal is modulated. By cross-correlating the received pseudo-random data sequence with a locally generated replica, the probe is capable of measuring the channel's impulse response, as well as its signal bit-error-rate (BER). Propagation measurements were made with the wideband probe at the same locations used for the earlier narrowband measurements in both deciduous and coniferous vegetation. A 28.8 GHz narrowband channel is operated in addition to the 30.3 GHz wideband channel to provide a means for comparison with the earlier narrowband data.

This report presents the results of the 28.8 GHz narrowband and 30.3 GHz wideband propagation measurements through deciduous vegetation. These deciduous vegetation measurements were made in April and August, 1990, with the trees in the defoliated and foliated states, respectively. The measurements were made at the pecan orchard near Wichita Falls, Texas, where the original narrowband deciduous vegetation measurements were made in 1982. The wideband propagation measurements, through coniferous vegetation, were made in the fall of 1991.

In the deciduous measurements, the test paths used in the earlier measurements, were duplicated as closely as possible so that the wideband data could be compared with the narrowband data. Measurements were made over 15 different paths, with lengths ranging from 0.2 to 0.7 km., and with 1 to 24 trees on the path. Most of the measurements were made with the transmitter and receiver terminals carefully positioned such that a row of trees was directly in the path. Three sequences of measurements were made with an increasing number of trees on the path, starting at one tree. Two diagonal paths also were used, in which the transmitter and receiver terminals were placed such that the paths traversed several rows of trees in a somewhat random fashion. In each case, the transmitter and receiver locations were carefully noted to allow a replication of measurements with the trees in the foliated state. For each path, azimuthal and elevation scans were made with the receiver antenna, while the transmitter antenna remained fixed. During each scan, measurements were made of received signal level, bit-error-rate and impulse response on the 30.3 GHz wideband channel, and received signal level on the 28.8 GHz narrowband channel.

2. EQUIPMENT DESCRIPTION

The electronic equipment used to make the propagation measurements was housed in two vehicles which could be positioned in the orchard independently. The transmitter antennas and radio frequency (rf) electronics were mounted directly to a sturdy aluminum mast, which allowed the transmitter height to be varied between 0.5 and 5 meters. This mast was rigidly attached to a truck so that the transmitter

could be positioned anywhere in the orchard. The baseband transmission equipment was located in the bed of the truck to minimize the weight on the mast. The receiver antenna and rf electronics were mounted on a remotely controllable positioner on top of a van. This positioner permitted the receiver antennas to be scanned in either the azimuth or elevation planes. This van also housed the intermediate frequency (IF) sections of the receivers, the baseband signal processing equipment, and the data acquisition computer. Since the 28.8 GHz narrowband link and the 30.3 GHz wideband link utilize very closely separated transmitter antennas and the same receiver antenna (with orthogonal polarizations), they travel over nearly the same path and experience nearly the same obstructions. All of the transmitter and receiver electronics were housed in thermostatically controlled, electrically shielded boxes (a constant enclosure temperature is necessary to minimize the amplitude and frequency drift of the rf electronics).

The transmitter configuration is diagrammed in Figure 2.1. In order to maintain phase coherency among the transmitted signals, a single 100 MHz temperature compensated crystal oscillator (TCXO) was used as a reference for all of the transmitters. In addition to the 28.8 and 30.3 GHz millimeter-wave links, an 11.4 GHz microwave link was also operated during the measurements. This link, which was physically separate from the other links, was used to maintain a phase-locked condition between the TCXO at the transmitter and the local oscillator (LO) reference source at the receiver.

At the transmitter, the 11.4 GHz signal was derived from the 100 MHz reference by means of a cavity-tuned x114 multiplier. The multiplier output of 40 mW fed a 46 cm parabolic dish antenna. The 28.8 GHz signal was generated from the 100 MHz reference by a cavity-tuned x96 multiplier followed by a varactor tripler. The output of the tripler (2 mW) injection-locked a Gunn diode oscillator through a high-isolation ferrite circulator. The Gunn output was split by a 3 dB directional coupler, feeding 60 mW at 28.8 GHz to a horizontally polarized, 24.5 dB gain rectangular horn antenna and 60 mW to a wideband upconverter, where it acted as a carrier for the 30.3 GHz signal.

The wideband subcarrier signal was generated by binary phase-shift keying (BPSK) modulation of a 1.5 GHz carrier with the 500 Mb/s pseudorandom word generator output. The 1.5 GHz subcarrier was then fed to the wideband upconverter along with the 28.8 GHz carrier. The upconverter output (1.5 mW) was then amplified by a Ka-band power amplifier with a high degree of amplitude flatness and phase linearity. After amplification, the 200 mW 30.3 GHz wideband signal was fed to a vertically polarized 24.5 dB gain rectangular horn antenna. A summary of the transmitter characteristics appears in Table 2.1.

A block diagram of the receiver appears in Figure 2.2. All LO signals used in the downconversion process were derived from a 99.95614 MHz, voltage-controlled crystal oscillator

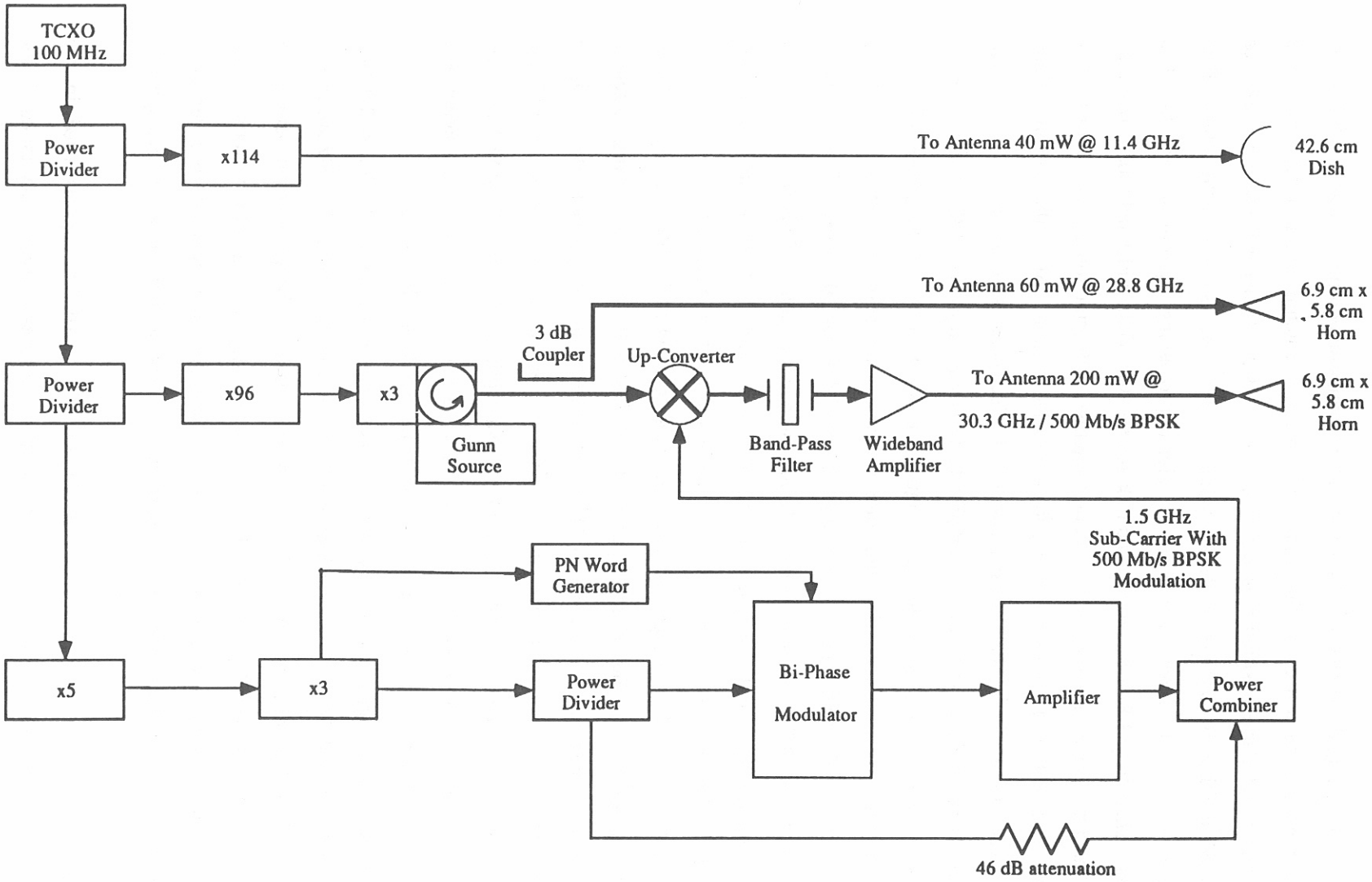

Figure 2.1. Block diagram of the transmitter equipment.

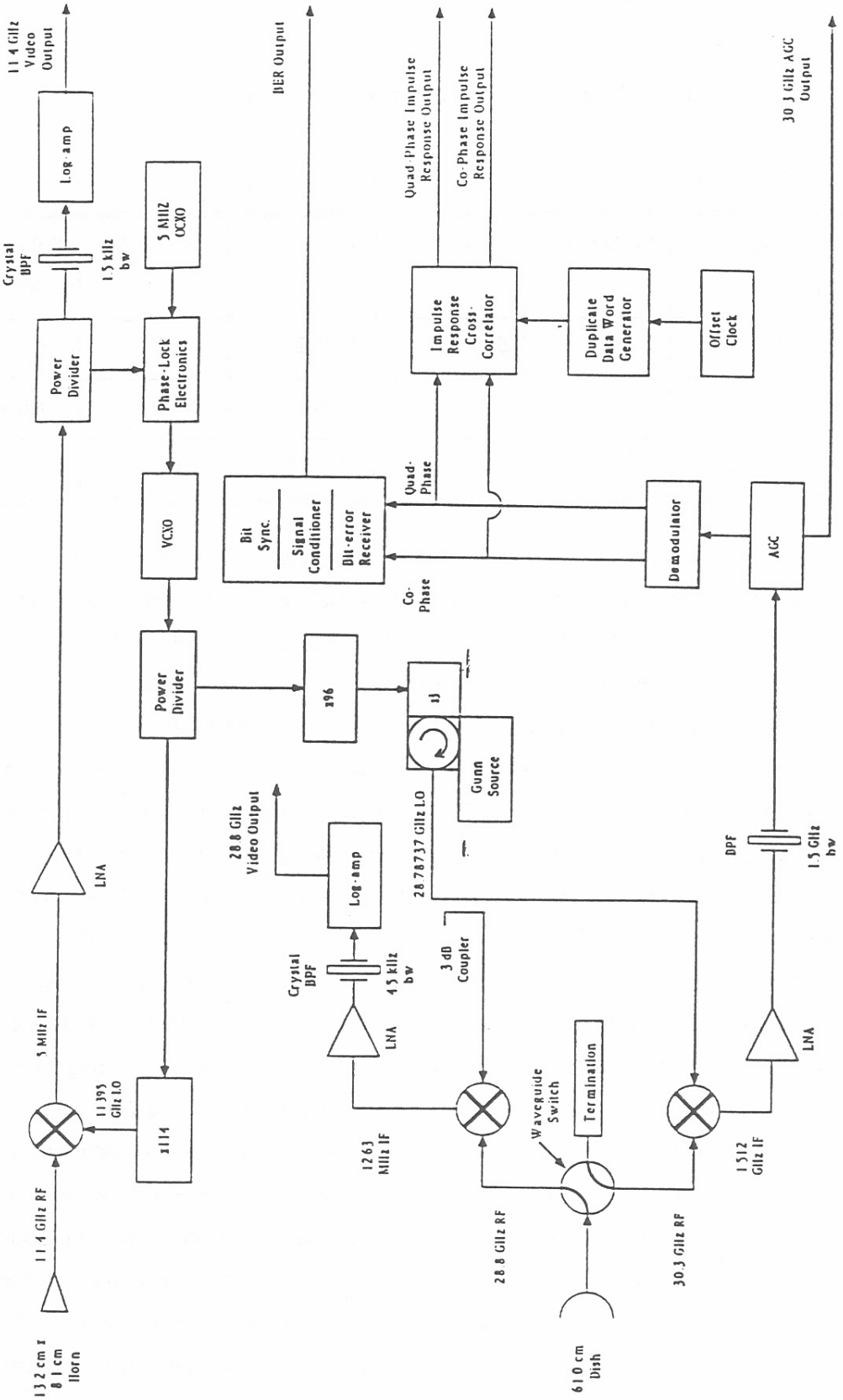

Figure 2.2. Block diagram of the receiver equipment.

Table 2.1. Summary of Transmitter Characteristics

----------Transmitter---------- ----------Antenna----------

Frequency	Power	Modulation	Type	Gain	Beamwidth	Polari-zation
11.4 GHz	40mW	cw	dish	32.5dB	4.2°	vertical
28.8 GHz	60mW	cw	horn	24.5dB	10.7°	horizontal
30.3 GHz	200 mW	BPSK	horn	24.5 dB	10.7°	vertical

(VCXO), which was phase-locked to the received 11.4 GHz signal. The phase-locking of the LO reference ensured phase coherency between the receiver IF signals and the transmitted signals.

The 99.95614 MHz VCXO reference, after passing through a x114 multiplier, yielded an 11.395 GHz LO signal. The incoming 11.4 GHz signal, which was intercepted by a 19.0 dB gain rectangular horn antenna, was mixed with this LO signal to produce a 5 MHz IF for the 11.4 GHz link. The incoming 28.8 and 30.3 GHz signals were intercepted by a 61 cm parabolic dish antenna. A 28.78737 GHz LO was generated for the 28.8 GHz link by means of an x96 multiplier followed by a varactor tripler and an injection-locked Gunn diode oscillator, yielding a 12.63 MHz IF for the 28.8 GHz link. These IF's, after passing through low-noise preamplifiers, were fed into narrowband crystal filters, and then to ac-to-dc logarithmic amplifiers (log-amps). The log-amps converted the IF signals to dc voltages, which were logarithmically proportional to the received RF signal amplitudes. The log-amps have an 80-dB dynamic range, with linearity of + /- 0.5 dB. The 28.78737 GHz LO used in the 28.8 GHz downconverter also was used as an LO in the 30.3 GHz downconverter, yielding a 1.512 GHz wideband IF signal. A summary of the receiver characteristics appears in Table 2.2.

After being downconverted, the wideband IF signal was then demodulated to produce the received 500 Mb/s baseband data stream. The baseband data were then sent to either the BER receiver or to the impulse response circuitry, depending on the measurement being made. In order to make a measurement of the impulse response of the channel, the clock rate for the duplicate data word would be offset from that of the received data word so that the two data words could be "slipped" past one another. The two data words would then be fed into a cross-correlator. Under these conditions, the cross-correlator produced a periodic impulse response measurement of the propagation channel.

Table 2.2. Summary of Receiver Characteristics

----------Receiver----------				----------Antenna----------		
Frequency	Bandwidth	Noise	Type	Gain	Beamwidth	Polarization
11.4 GHz	1.5 kHz	7.5 dB	horn	19.0 dB	20.0°	vertical
28.8 GHz	4.5 kHz	7.5 dB	dish	42.5 dB	1.3°	horizontal
30.3 GHz	1000 MHz	8.0 dB	dish	43.0 dB	1.2°	vertical

A more detailed description of the electronics used in the wideband 1.5 GHz demodulator, the BER receiver, and the impulse response circuitry, can be found in the NTIA report "A Diagnostic Probe to Investigate Propagation at Millimeter Wavelengths" (Violette, et al., 1983). Data acquisition, processing, and storage were carried out on a personal computer equipped with a 12-bit analog-to-digital (A/D) interface.

3. MEASUREMENTS

The segment of the Chitwood-Montz pecan orchard near Wichita Falls, Texas, used for the 1982 narrowband measurements, was also used for the 1990 narrowband and wideband measurements. This orchard, which was originally selected for its uniformity, was an established and well-groomed stand of trees. It was selected to permit the measurement of propagation data as a function of only the trees of interest, and not of other vegetation. This uniform tree density also allows the dependence of received signal parameters with foliage depth to be determined as accurately as possible. The orchard had changed somewhat between the years of 1982 and 1990. Several of the trees had been removed from the orchard during this period. However, the test paths for the 1990 measurements were carefully chosen to be as close to those used in the 1982 measurements as possible.

3.1. Orchard Layout

The orchard consists of several thousand well-groomed pecan trees, all of the same age, which have been planted in a square grid pattern. The spacing between trees is approximately 13 meters, and the trees range in height from 8 to 10 meters. The maximum length of branches reached 10 to 13 meters, filling the space between rows in many areas. The initial branching occurs at the 1.5 to 2.0 meter height,

with significant branching at the 4 to 6 meter level. There are few branches, mainly trunks, at the 1.0 meter level. The leaves of the pecan trees grow in clusters of 10 to 12 leaves on each twig. The leaves are arranged on the twigs symmetrically, and range in size from 5 cm long and 2 cm wide near the branch to 20 cm long and 5 cm wide at the end of the twig. In April, during the defoliated measurements, a grain crop planted as a temporary ground-cover had attained a height of 2 to 5 cm, providing a clean-looking ground plane free of weeds and underbrush.

The pictures in Figure 3.1 were taken of the orchard in early April, 1990. Picture (a) shows the receiver van positioned with three trees on path. The uniform planting of the trees is evident from this picture. Picture (b) was taken in between tree rows. It also shows the receiver van positioned in the orchard with several trees on path. In picture (c), the transmitter is shown at its usual location, across the open field from the edge of the orchard.

In August, the trees were in full leaf and the nuts had grown to nearly full size. The ground-cover had grown to a height of 50 to 80 cm. The ground-cover was somewhat sparse within the orchard, but was quite thick in the open field where the transmitter was usually located. The pictures in Figure 3.2 were taken of the orchard in August, 1990. These pictures were taken in the same locations as the corresponding pictures in Figure 3.1. The difference in the vegetation density between these two sets of pictures is evident.

3.2. Path Description

The drawing in Figure 3.3 shows the portion of the pecan orchard in which the measurements were made. The numbered sites on the drawing are transmitter and receiver locations. The orchard was originally planted in a uniform grid, with a 13 meter spacing between tree trunks. Much of this grid remains; however, as indicated by the open spaces, some trees have been removed. Four major paths, 1, 2, D, and R, are indicated on the drawing.

On Path 1, data sets were recorded with the transmitter at Site 1 and with the receiver sequentially at Site 2 through Site 9. This measurement mode provided data sets with increasing foliage density as the sequence progressed. The data sets are indicated in Table 3.1 by path name. The first set on Path 1 is named CAL, and is a calibration path. The transmitter was at Site 1 and the receiver at Site.2. No trees are on this portion of the path. The other seven data sets on path 1 have file names, 1PA, 3PA, 8PA, 11PA, 14PA, 20PA, and 24PA. The transmitter and receiver locations, path type, path length, the equivalent number of trees, and the vegetation depth are given for each data set. The other three major paths are: Path 2, with the transmitter at Site 10 and the receiver at Sites 11, 12, 13, and

a)

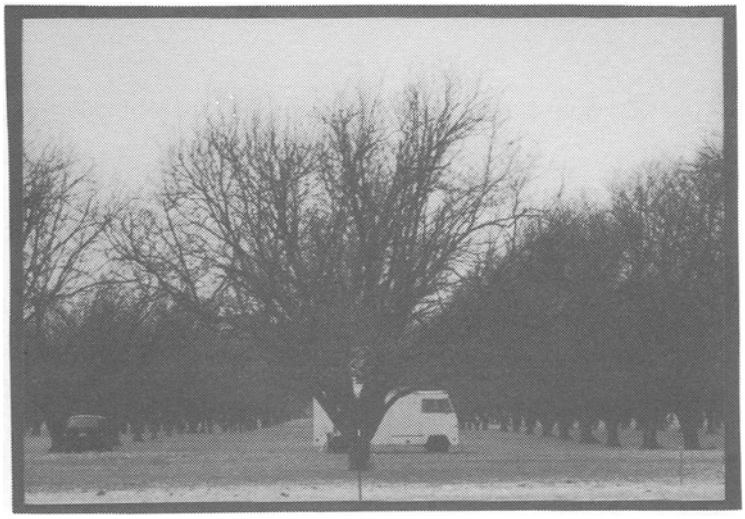

b)

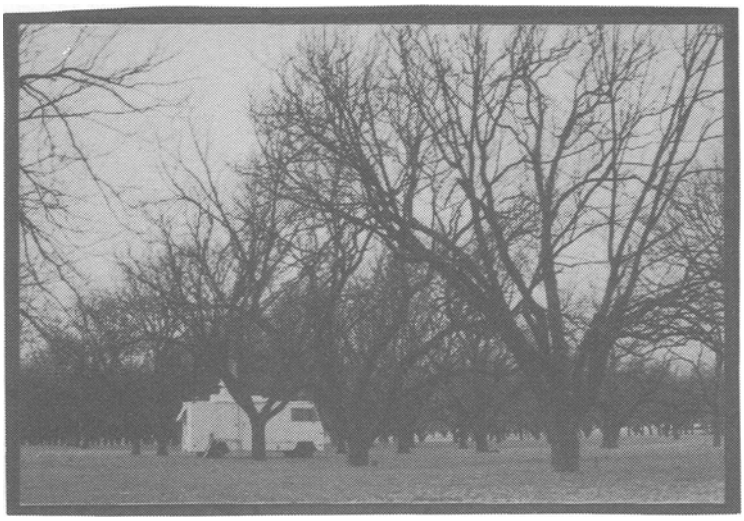

c)

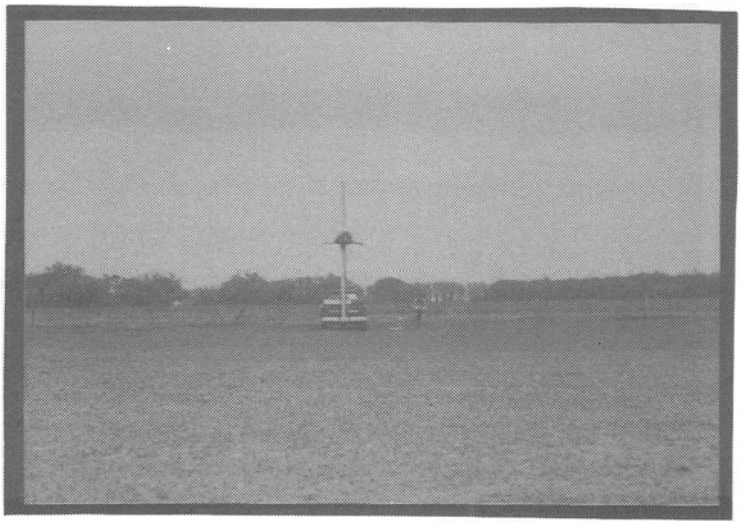

Figure 3.1 Photographs of pecan orchard in the defoliated state.

a)

b)

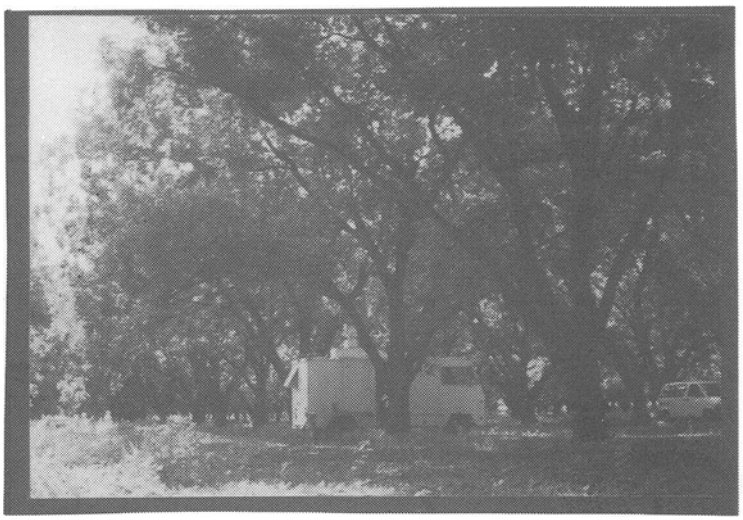

c)

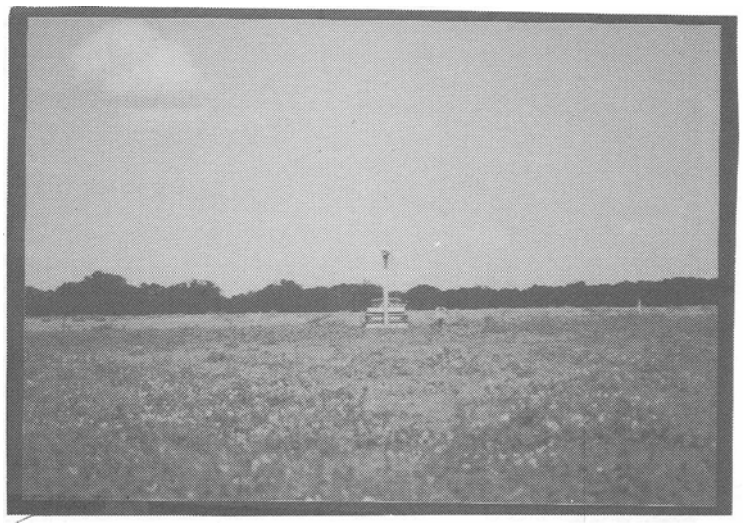

Figure 3.2 Photographs of pecan orchard in the foliated state.

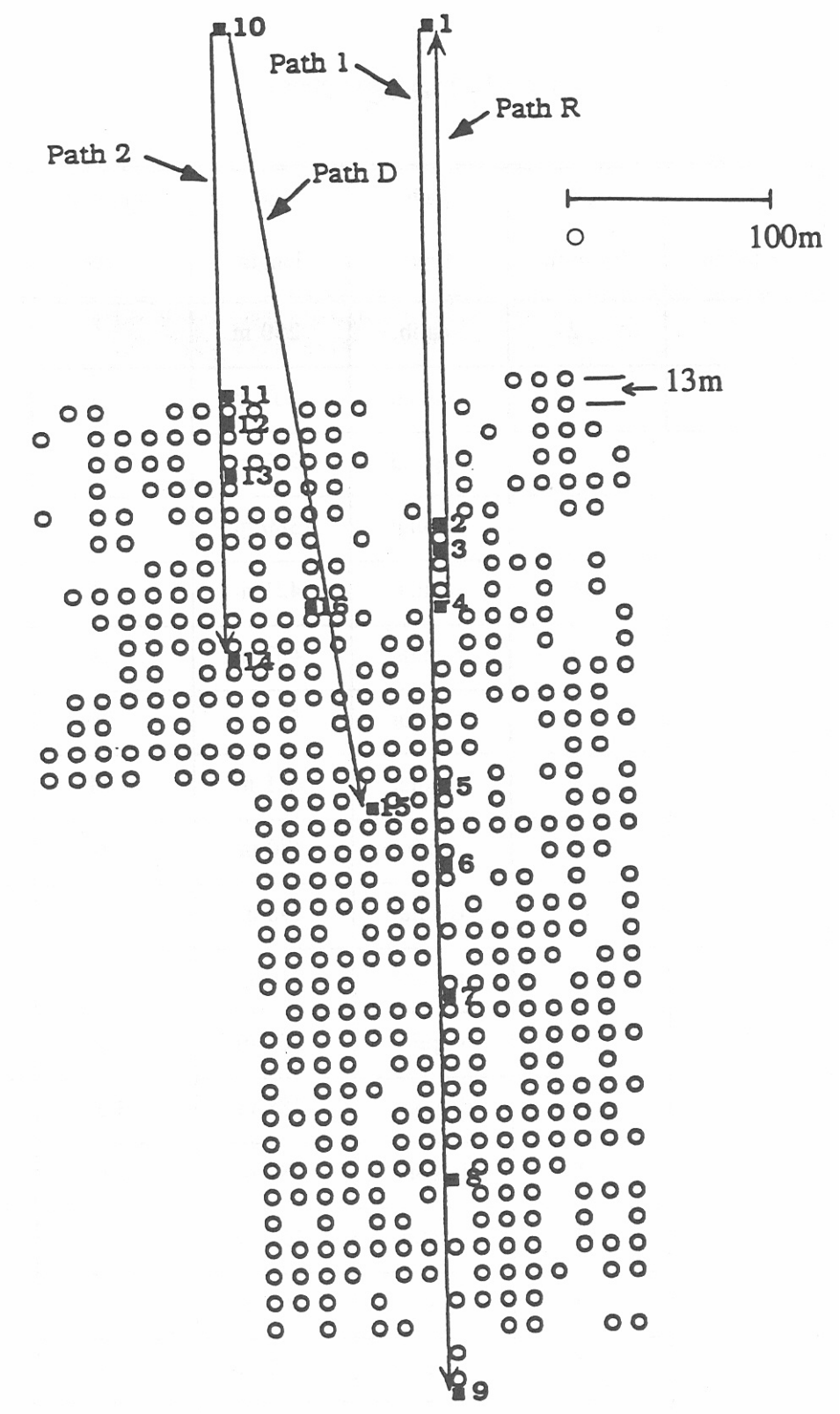

Figure 3.3. Diagram of pecan orchard layout.

Table 3.1. Path Descriptions

path name	TX location	RX location	path type	path length	equiv. # of trees	veg depth
CAL	1	2	calib.	250 m	0	0 m
1PA	1	3	regular	263 m	1	9 m
3PA	1	4	regular	292 m	3	27 m
8PA	1	5	regular	380 m	8	12 m
11PA	1	6	regular	421 m	11	99 m
14PA	1	7	regular	487 m	14	126 m
20PA	1	8	regular	577 m	20	180 m
24PA	1	9	regular	681 m	24	216 m
2CAL	10	11	calib.	180 m	0	0 m
1PB	10	12	regular	190 m	1	9 m
3PB	10	13	regular	216 m	3	27 m
8PB	10	14	regular	307 m	8	12 m
15D	10	15	diagonal	388 m	3.3	29.7 m
8D	10	16	diagonal	282 m	1.8	16.2 m
3CAL	2	1	calib.	250 m	0	0 m
1R	3	1	reverse	263 m	1	9 m
3R	4	1	reverse	292 m	3	27 m
8R	5	1	reverse	380 m	8	12 m

14; Path D, with the transmitter at Site 10 and the receiver at Sites 15 and 16; and Path R, with the receiver at Site 1 and the transmitter at Sites 2, 3, 4, and 5. Note that Path D looks diagonally across the orchard grid and Path R is a repeat of Path 1 with the transmitter and receiver locations interchanged for the first four data sets of Path 1.

As the transmitter and receiver were positioned at each of the location pairs which define a path, a data set was recorded. Each data set consisted of an azimuthal scan of the 30.3 GHz receiving antenna within a ± 30° limit. At discrete angles within this limit, a signal level reading, a BER reading, and an impulse response were recorded. Typical angle sets are shown in the sample data to follow. Similarly, an elevation scan of the 30.3 GHz receiving antenna was made within a ± 10° limit of the receiving antenna. Also, at each receiver position on the path, continuous scans (within ± 15° azimuth and ± 10° elevation) were made with the 28.8 GHz receiving antenna. These data sets were recorded with the receiving antenna at a 4 meter height, and with the transmitting antenna at a 1 meter height, and again at 4 meters.

3.3. Calibrations and Field Data

In this section, samples of the recorded data from trees in a defoliated state are shown. The data in Figure 3.4 (a) show the 28.8 GHz received signal level (RSL) as a function of azimuth angle on Path 1, from -15° to +15°, with the transmitting antenna at the 4 meter height. During each scan, the transmitting antenna is aligned directly along the transmitter-receiver path. The 0° angle of the scan occurs when the receiving antenna is pointing directly at the transmitter. These data are part of the data set CAL identified in Table 3.1, and were recorded with the transmitter at Site 1 and the receiver at Site 2, as shown in Figure 3.3. The data in Figure 3.4 (b), show the received signal level at 30.3 GHz on Path 1 with the transmitting antenna at the 4 meter height. These data are similar to the 28.8 GHz data in Figure 3.4 (a), except that the scan width is limited to +/- 10°, and the signal levels were recorded at discrete angles as opposed to the continuous sampling in the 28.8 GHz data. The data in Figure 3.4 (b), were sampled at -10°, -8°, -6°, -5°, -4°, -3°, -2°, -1°, 0°, +1°, +2°, +3°, +4°, +5°, +6°, +8°, and +10°. The plotting routine gives a smooth-line connection of these points. These data are also part of the CAL data set. The data in Figures 3.4 (a) and 3.4 (b) provide a calibration reference for the remaining azimuthal scanned 28.8 GHz and 30.3 GHz data respectively, in the Path 1 group.

The data in Figure 3.4 (c) was recorded in a manner similar to that in Figure 3.4 (a). The only difference is that the data in Figure 3.4 (c) resulted from an azimuthal scan with one tree on the propagation path, and the signal amplitude in the figure is indicated as vegetation loss. Vegetation loss is used for all paths with trees. This terminology implies that all reduction in the received signal is the

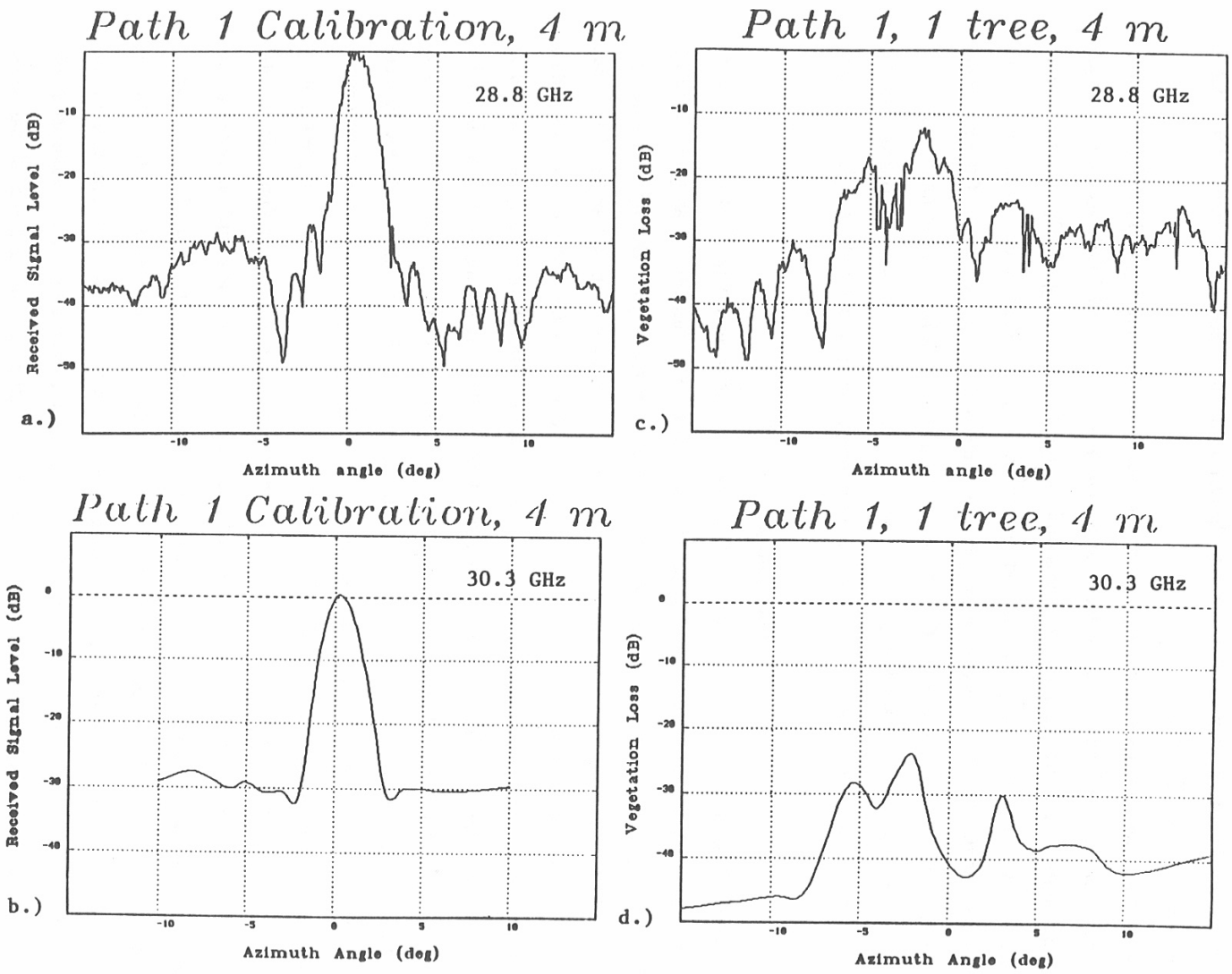

Figure 3.4. Received signal level and vegetation loss scans as a function of receiving antenna azimuth at 28.8 and 30.3 GHz.

6result of attenuation and scattering due to the tree foliage and not the result of signal reduction due to increased path length. Simply, the signal is normalized by the increased path length ratio. Likewise, Figure 3.4 (d) compares to 3.4 (b). The data in Figure 3.4 (d) resulted from measurements made with one tree on the path.

The data presented in Figures 3.5 (a), (b), (c), and (d) correspond, respectively, to the data in Figures 3.4 (a), (b), (c), and (d). The only difference is that the data in Figure 3.5 results from a scan of the receiver antenna in elevation, rather than in azimuth. The receiving antenna was scanned over the angle limits indicated in the figures.

At the 30.3 GHz frequency, for each recording of RSL or vegetation loss, a corresponding recording was made of the bit error rate. Samples of these data are shown in Figure 3.6. In Figure 3.6(a), the azimuthal scan data of Figure 3.4(b) is replotted and the corresponding bit error rate data for that scan is shown in Figure 3.6 (b). At each angle, the amplitude and bit error rate data were acquired sequentially. The data in Figures 3.6 (c) and 3.6 (d) are the vegetation loss (replotted from Figure 3.4(d) and the corresponding bit error rate data, respectively.

The third data type routinely recorded for each of the 30.3 GHz azimuthal and elevation scans was an impulse response record. Examples of these records are shown in Figure 3.7. By the sampling method described in Section 2 (Equipment Description), voltage levels representing the co-phase and quad-phase components of the impulse response were acquired and recorded. From these pairs of sampled data, the relative phase and impulse amplitude were calculated. This data set, (the cophase and quadphase components, relative phase and amplitude) was then plotted as a function of time, as shown in Figure 3.7. The plotting routine establishes an arbitrary zero point, such that the entire impulse and all delayed signal components are present. In Figure 3.7, the zero reference for determining component delay values is at the mid-point of the direct signal impulse. A time reference mark is shown in each of the four figures in the set. No significant delay components are present in Figure 3.7 (a), nor are any expected, because it was recorded on a calibration path. Also, the impulse in Figure 3.7 (b) shows no significant delay components. There are, however, delay components in both Figures 3.7 (c) and 3.7 (d). Delay components in Figure 3.7 (c) are at 1, 3, 9, and 14 ns (nanoseconds) relative to the reference mark, and in Figure 3.7 (d) are at 4, 11, and 15 ns relative to the reference mark.

For each data set on the four major paths, at selected receiver antenna angle positions, the received signal IF frequency spectrum was recorded. Examples of these spectra are shown in Figures 3.8(a) and (c). Examples of impulse response data recorded at corresponding antenna positions are shown in Figures 3.8 (b) and (d). The spectrum-impulse response set in Figures 3.8 (a) and (b) is

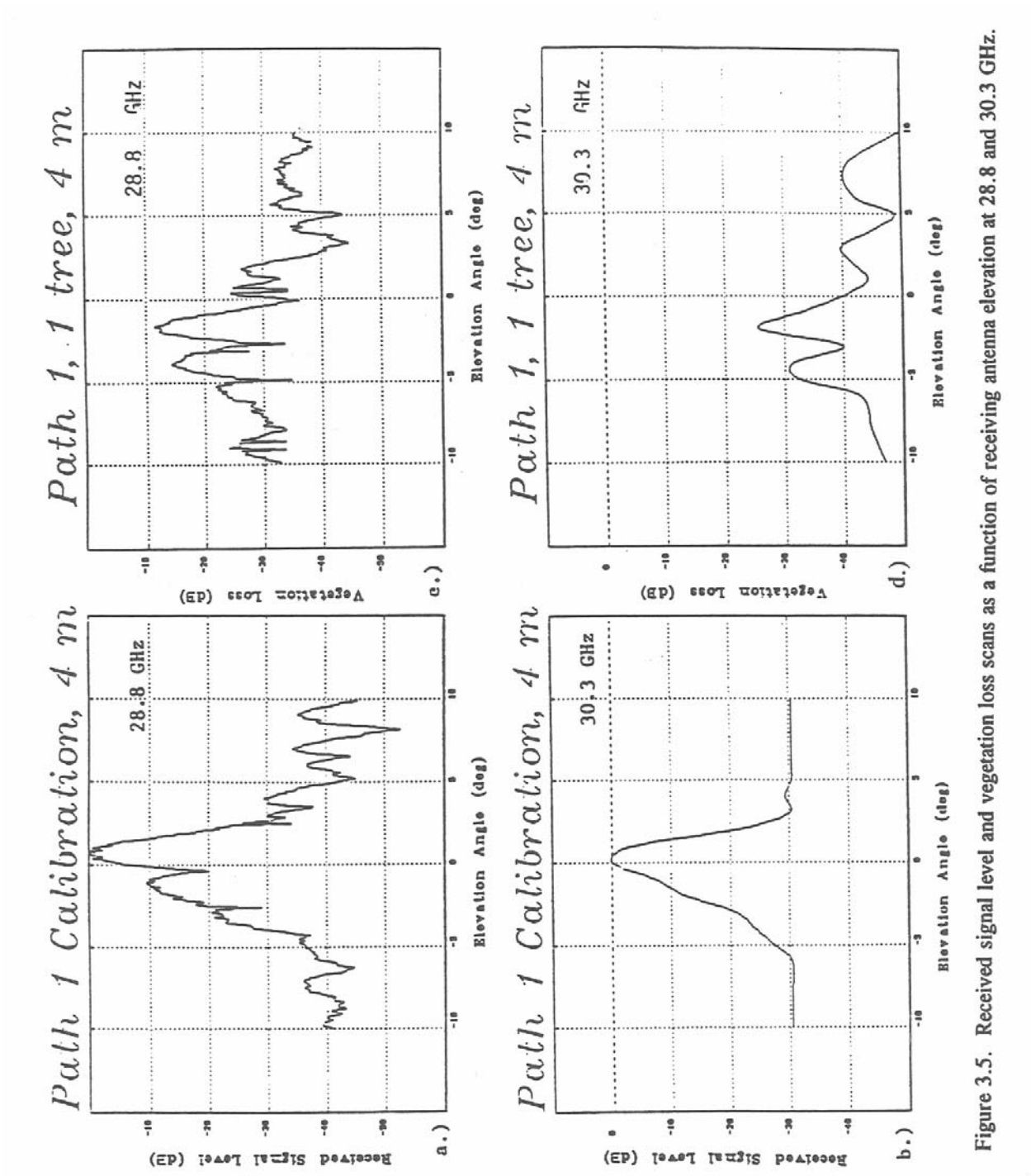

Figure 3.5. Received signal level and vegetation loss scans as a function of receiving antenna elevation at 28.8 and 30.3 GHz.

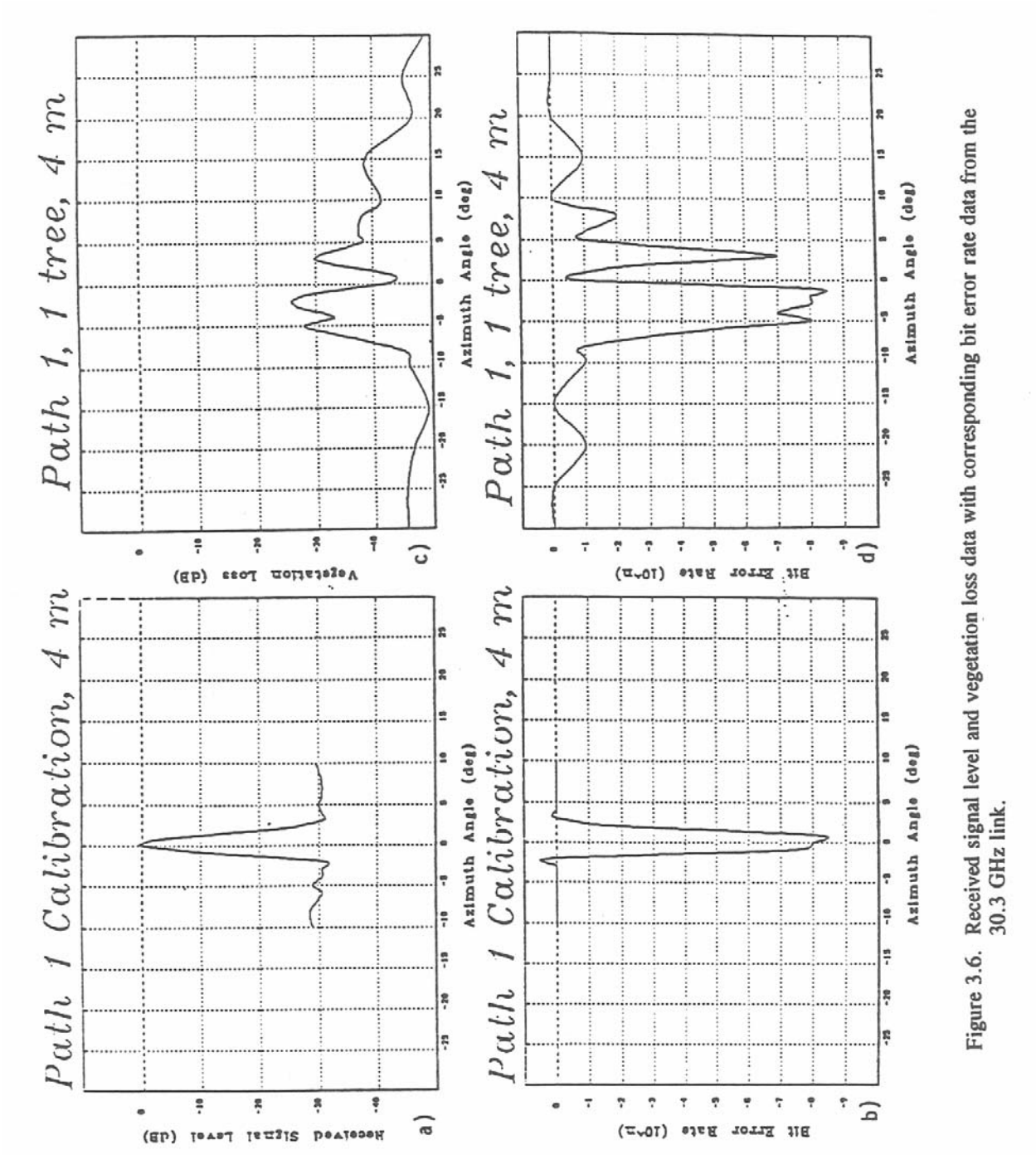

Figure 3.6. Received signal level and vegetation loss data with corresponding bit error rate data from the 30.3 GHz link.

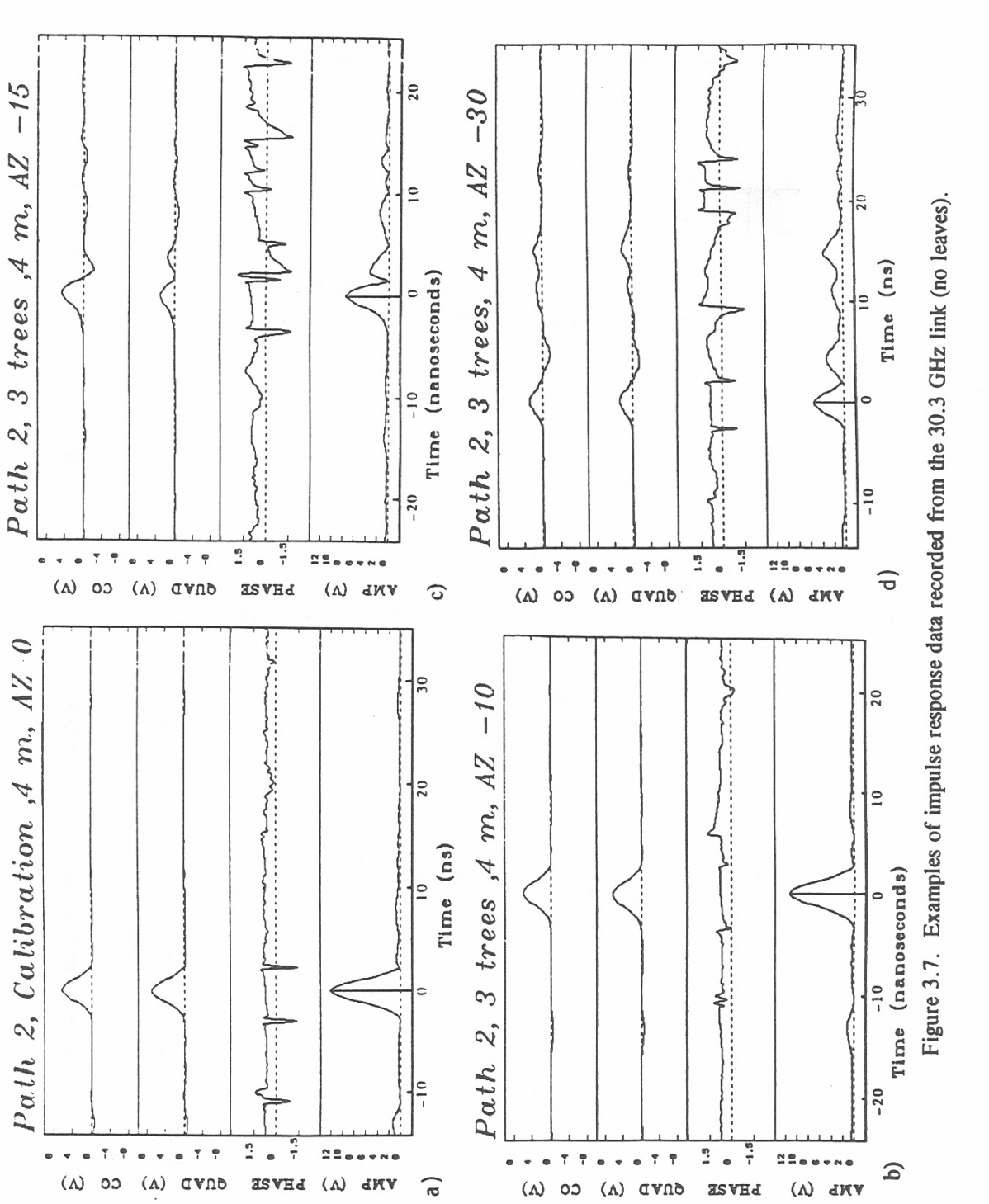

Figure 3.7. Examples of impulse response data recorded from the 30.3 GHz link (no leaves).

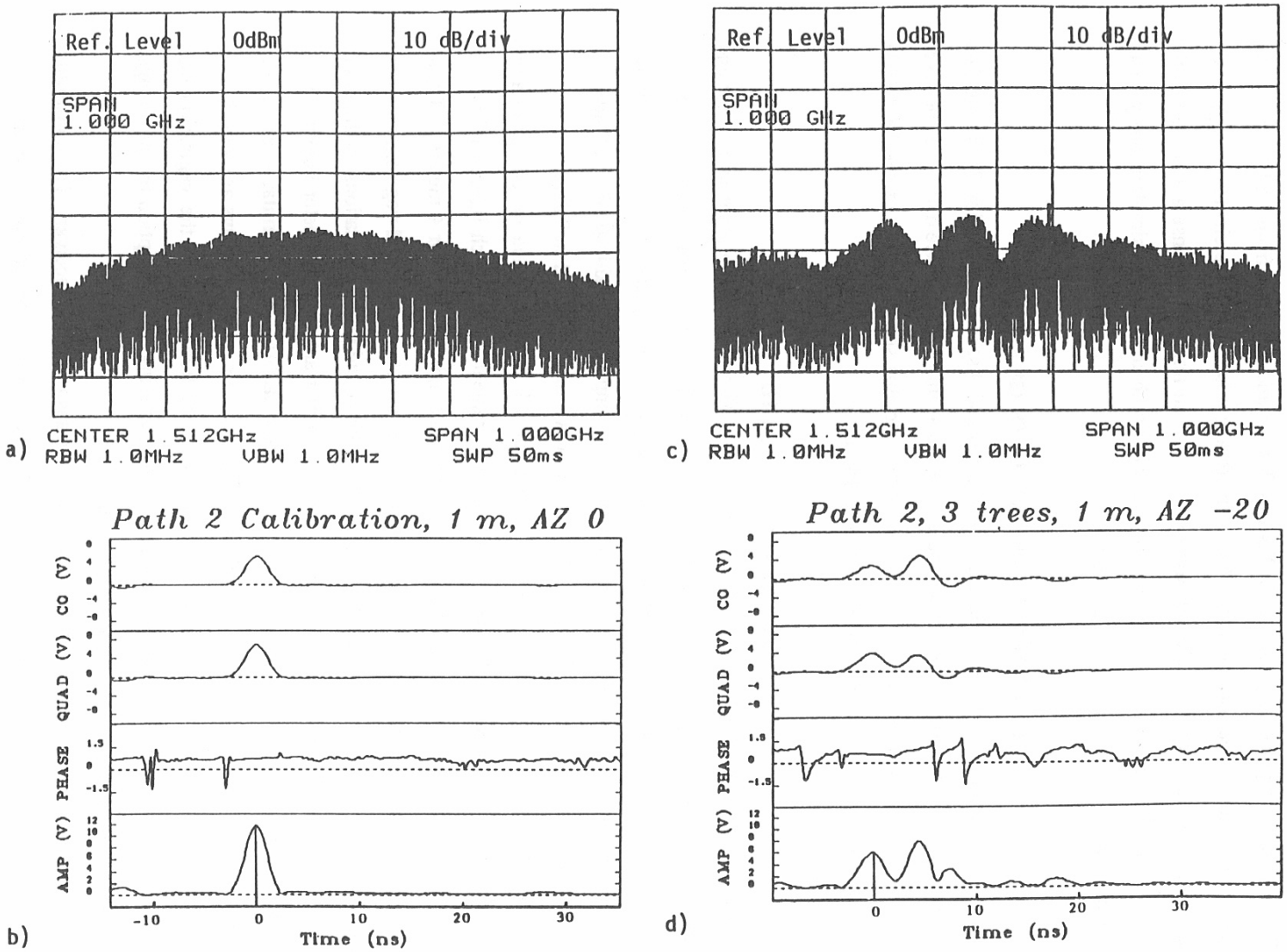

Figure 3.8. Examples of frequency spectra and corresponding impulse response data from the 30.0 GHz link.

from the Path 2 calibration at 1 meter transmitter height, with 0° azimuthal pointing and 0° elevation pointing. The spectrum-impulse response set in Figures 3.8 (c) and 3.8(d) is from Path 2 at 1 meter transmitter height with three trees on the path. The azimuth angle is -20 and the elevation angle is 0°. The amplitude and time delay of the multipath signals shown in an impulse response are related to the amplitude and spacing of the nulls in the frequency spectra, when both are recorded simultaneously. This relationship is discussed in more detail in Section 5.

4. DATA ANALYSIS AND RESULTS (28.8 GHz)

Examples of five types of recorded data were presented and discussed in Section 3. These data types (amplitude data at 28.8 GHz and amplitude data, BER data, impulse response data, and spectrum scans at 30.3 GHz) were recorded at each of the path sites. In this section, some of the 28.8 GHz records are presented for analysis and comparison to the 1982 data.

4.1 Amplitude Data at 28.8 GHz

The amplitude data at 28.8 GHz was obtained from azimuth and elevation scans at 1 meter and 4 meter transmitter antenna heights for the various numbers of trees on several paths described in Section 3. Examples of the azimuth scans were shown in Figures 3.4 (a) and (c); examples of the elevation scans were shown in Figures 3.5 (a) and (c). Several composites of additional amplitude data at 28.8 GHz are shown in Figures A.1 through A.8 (Appendix A), and are listed in Table 4.1.

The data in these figures (A1 through A8) are from Paths 1, 2, and R, and include calibration and measurements at 1 tree, 3 trees, and 8 trees. From a measurement setting, each figure differs only in scan angle (azimuth or elevation) and/or in transmitter antenna height (1 meter or 4 meters). These data composites were made to enable comparisons emphasizing the effects of increased vegetation on path and the pattern difference resulting from interchanging the transmitter and receiver locations on the same path. The data in Figure A.1 are azimuthal scans with the transmitter antenna at 1 meter height. The first column consists of calibrations on Paths 2, 1, and R. These calibrations are similar -- essentially the antenna pattern of the receiving antenna is displayed. The remaining three columns are with 1 tree, 3 trees, and 8 trees on path. The differences between the calibration RSL and the vegetation loss measurements are the reduced peak signal in the scan, due to scattering and absorption by the foliage, and the broadening of the pattern as a function of scan angle.

Paths 1 and 2 are similar regarding the placement of the transmitter and receiver. The transmitter is in the open field and the receiver is in the orchard. For Path R, however, the receiver is in the open

Table 4.1. Amplitude Scan Data at 28.8 GHz

Figure Number	Scan Azimuth/Elevation	Transmitter Height (Meters)	Foliage State Leaves/No Leaves
A.1	Azimuth	1	No Leaves
A.2	Azimuth	4	No Leaves
A.3	Elevation	1	No Leaves
A.4	Elevation	4	No Leaves
A.5	Azimuth	1	With Leaves
A.6	Azimuth	4	With Leaves
A.7	Elevation	1	With Leaves
A.8	Elevation	4	With Leaves

field and the transmitter is in the orchard. The results from paths 1 and 2 show no characteristics that can be uniquely attributed to either path. However, when comparing Path 1 and Path R, unique characteristics in the scan pattern are apparent. In the Path R patterns, much less broadening is observed. On Path 1, the 100 transmitting antenna is set back 250 meters from the first tree and the 1.2° receiving antenna is set back 5 meters from the first tree. In this mode, the transmitter illuminates approximately On the same physical path, but with the terminal positions reversed, Path R, the 10° transmitter antenna illuminates only a few meters at the first tree, and the narrow beam receiving antenna scans this much narrower illuminated region. The resulting scan patterns support this scenario. The scan patterns described above are apparent in the remaining 28.8 GHz data.

The data in Figure A.2, has the same format as that in Figure A.1. These data were recorded with the transmitter antenna at 4 meters above ground. The main difference between these data and those in Figure A.1, is seen in the even greater contrast between the Path 1 and Path R results. Also, there is slightly greater overall attenuation in the peak signals (except for the calibration data in Figure A.2) because of the increased foliage at the 4 meter height.

The data in Figures A.3 and A.4 have the same format as that in Figures A.1 and A.2. The

difference in the measurements is that elevation scans of +/-10° are used instead of azimuth scans. The patterns are quite similar to the azimuthal scans of Figures A.1 and A.2, except for the ground reflected component in the negative angle portion of the scan. This component is particularly apparent at about -2° in the calibration records for all paths, being most prominent in the 4 meter height data of Figure A.4. The data for 3 trees on Path 1, in Figure A.3. was not available.

The data and format of Figures A.5 through A.8 are similar respectively to the data and format of Figures A.1 through A.4. The data in Figures A.1 through A.4 were recorded in April when there were no leaves on the trees, and the data in Figures A.5 through A.8 were recorded in August, when the trees were in full leaf. The primary observation in comparing the two data sets, is the increased overall vegetation loss associated with the increased foliage for Figures A.5 through A.8 (trees with leaves). Also the scan pattern broadening in the Path 1 data when compared to the Path R data is again very apparent.

The data in Figures 4.1, 4.2, and 4.3 are the results of plotting peak amplitudes from the azimuth and elevation scans from Paths 1 and R. These plots emphasize the comparison of Path 1 vs. Path R differences and the vegetation loss differences with leaves and without leaves. The data in Figures 4.1 and 4.2 (measured at a transmitter height of 1 and 4 meters respectively) clearly show the approximate 10 dB less vegetation loss measured on the reverse path (Path R) compared to Path 1. This is due to the relative proximity of the transmitter to the tree locations (250 meters on Path 1 and 5 meters on Path R). Also apparent in these figures is the increased vegetation loss (overall in the order of 10 dB) associated with the increased foliage density (leaves on the trees).

The data in Figure 4.3 is a composite of the data in Figures 4.1 and 4.2. The results from the 1 and 4 meter transmitter heights were combined. This figure more clearly shows the effects of path orientation (Path 1 vs. Path R), and increased foliage (no leaves - April data vs. leaves - August data).

The last two figures in this section (Figures 4.4 and 4.5) compare the vegetation loss with trees on path from measurements taken in 1982 (upper figure) with data from the 1990 measurements (lower figure). There are two differences in the experimental conditions between the measurements. The first is that the receiver was fixed at 4 meters height for the 1990 data, whereas in the 1982 measurements both the receiver and the transmitter were at 1 meter for the 1-meter data and at 4 meters for the 4-meter data. The second difference is that, although the paths were the same (in number of trees on path), the actual trees differed slightly due to growth, pruning and removal of dead trees during the eight year time lapse between measurements. The results are generally compatible with a slightly greater loss rate observed

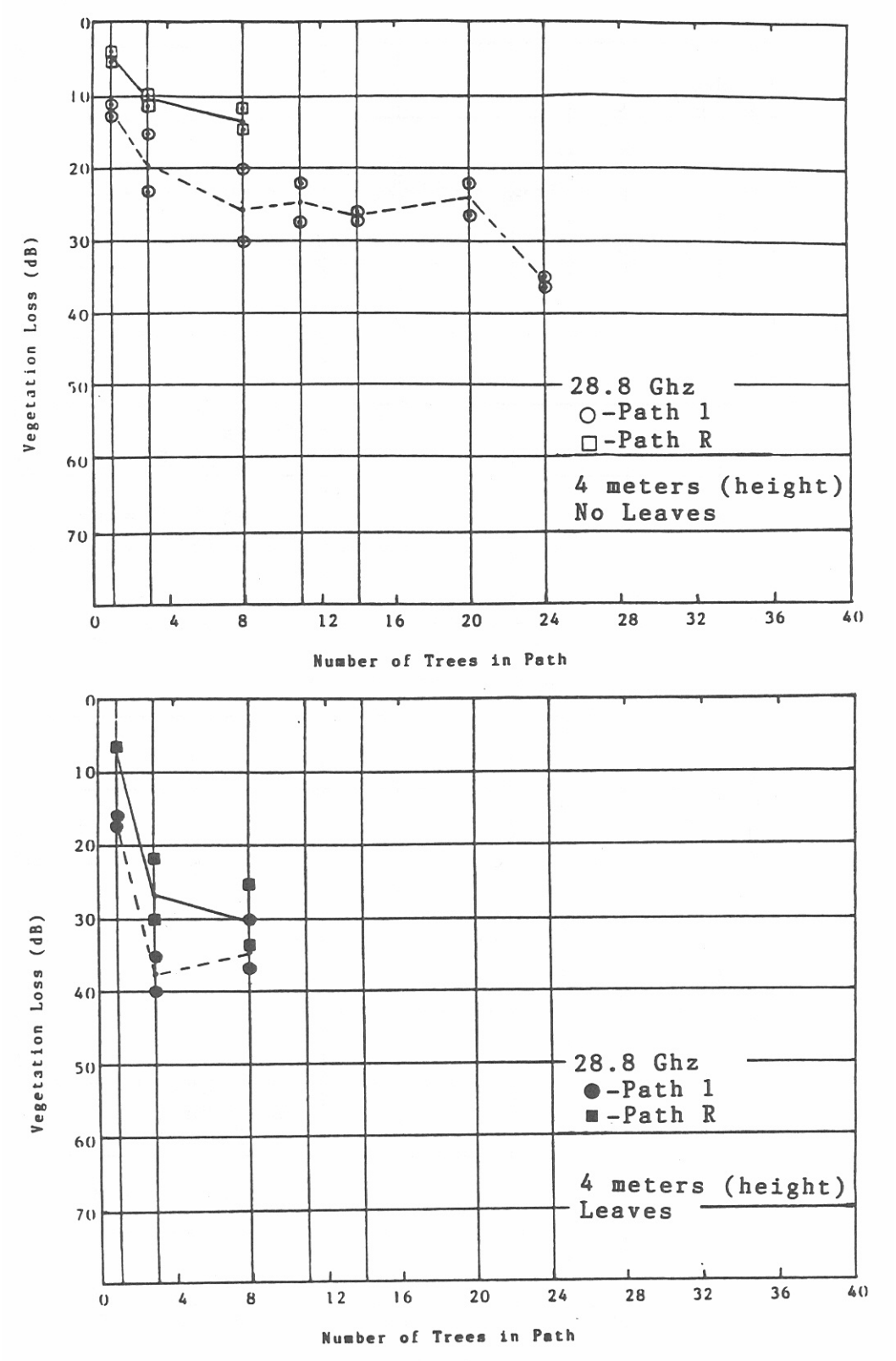

Figure 4.1. Vegetation loss values as a function of trees on path (the connecting lines indicate average values). Measurements at 1 meter transmitter height.

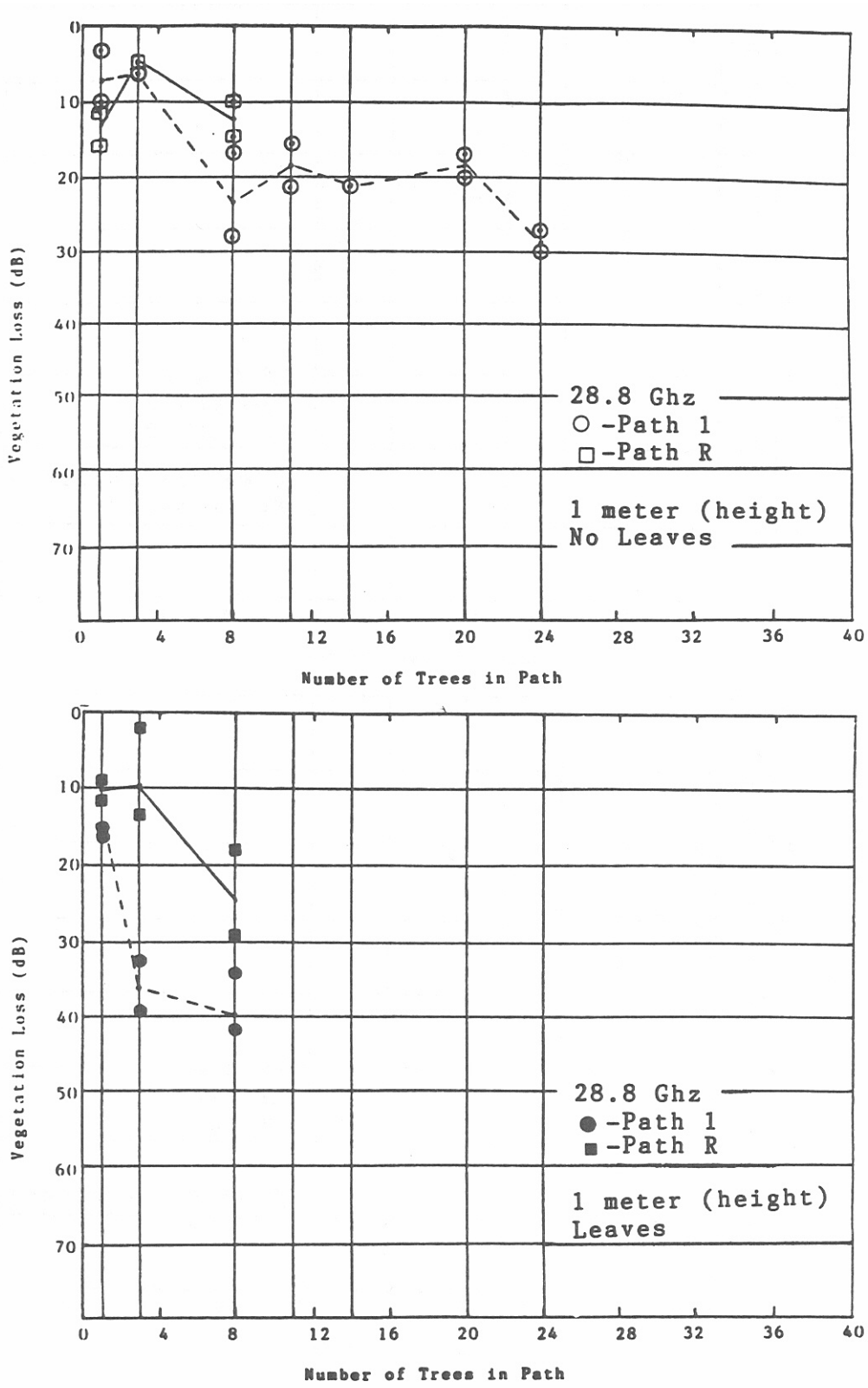

Figure 4.2. Vegetation loss values as a function of trees on path (the connecting lines indicate average values). Measurements at 4 meters transmitter height.

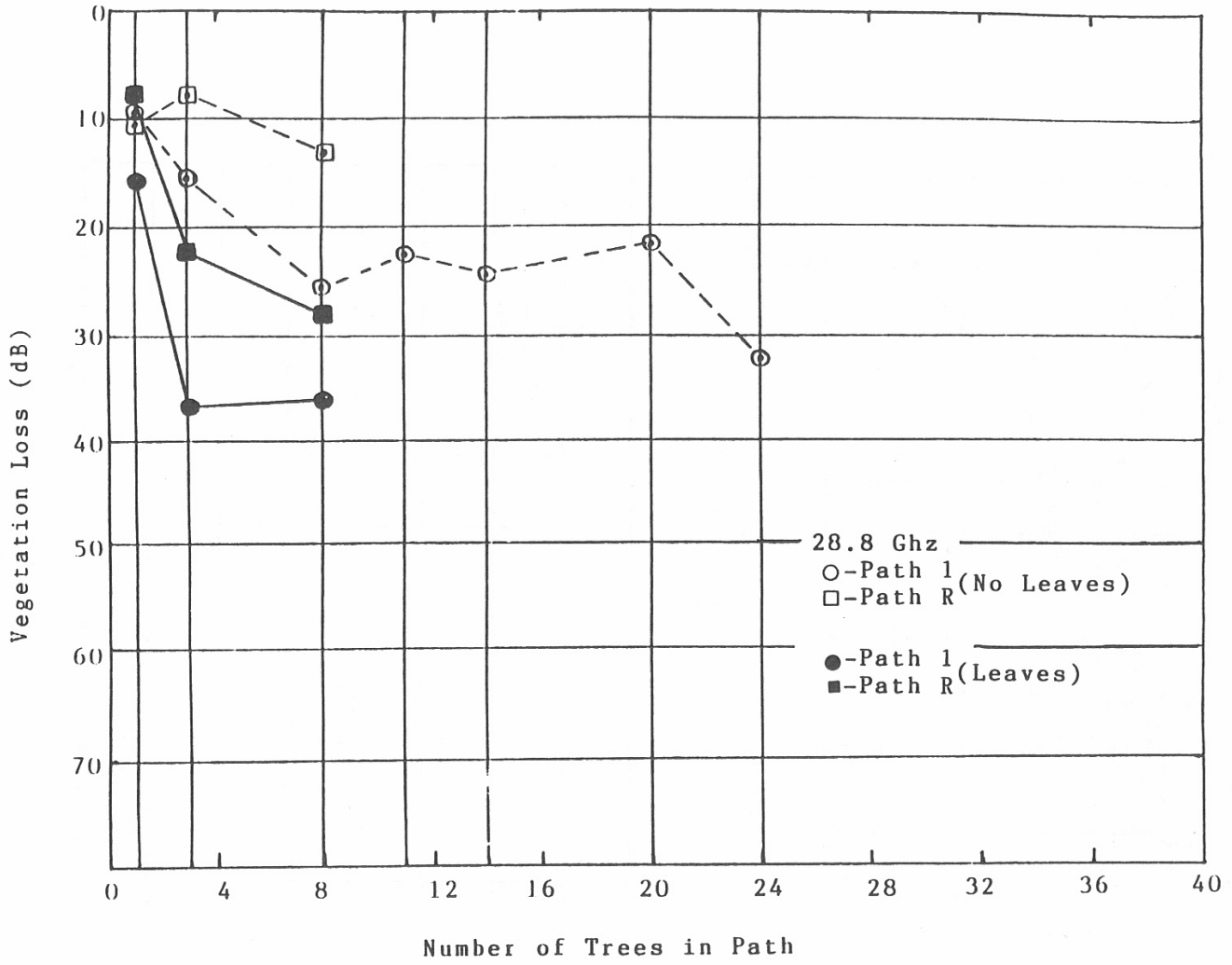

Figure 4.3. Vegetation loss values as a function of trees on path. These values are the average of the 1-meter and 4-meter transmitter height data.

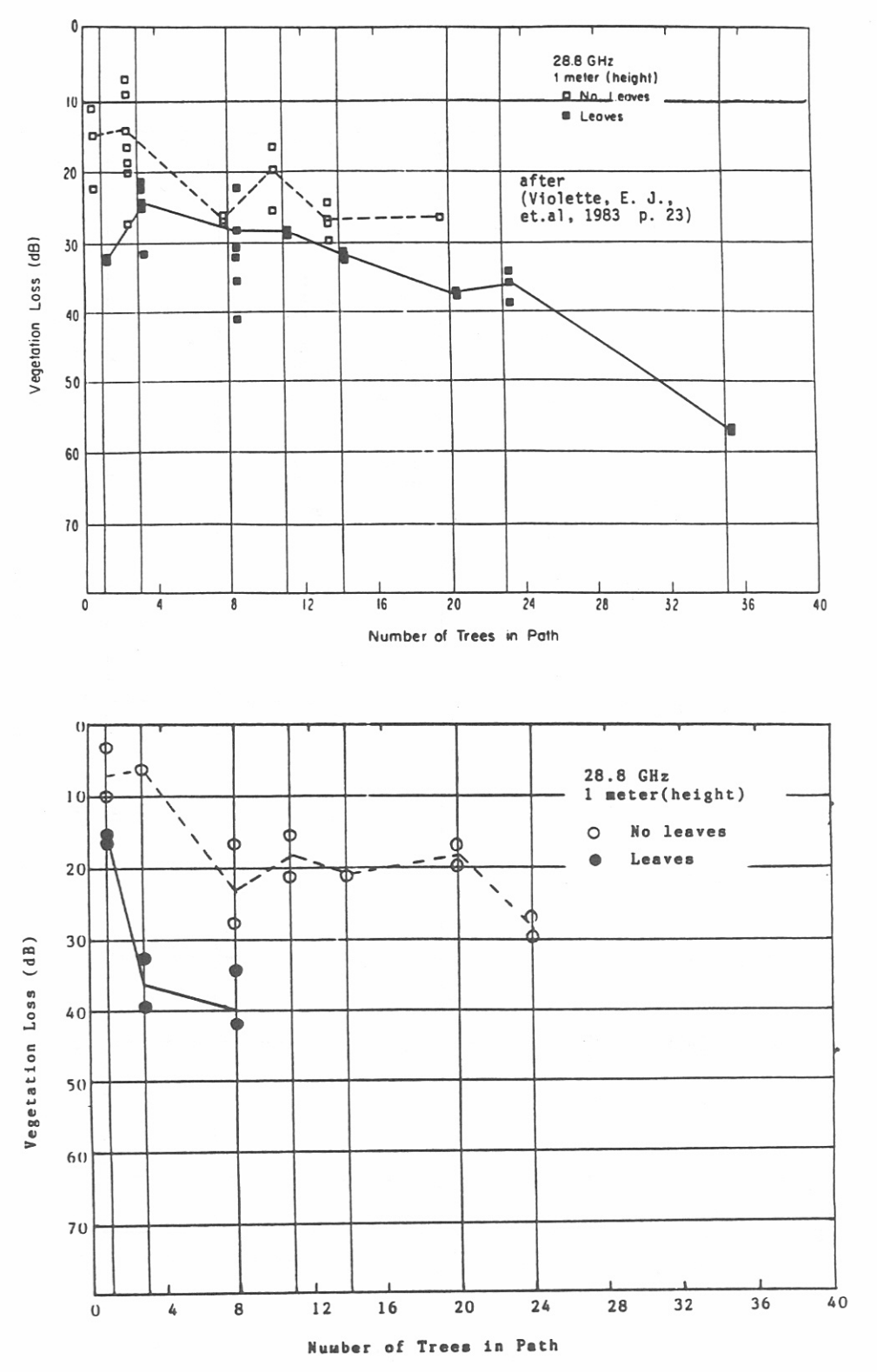

Figure 4.4. Vegetation loss as a function of the number of trees on path for 28.8 GHz at 1 meter.

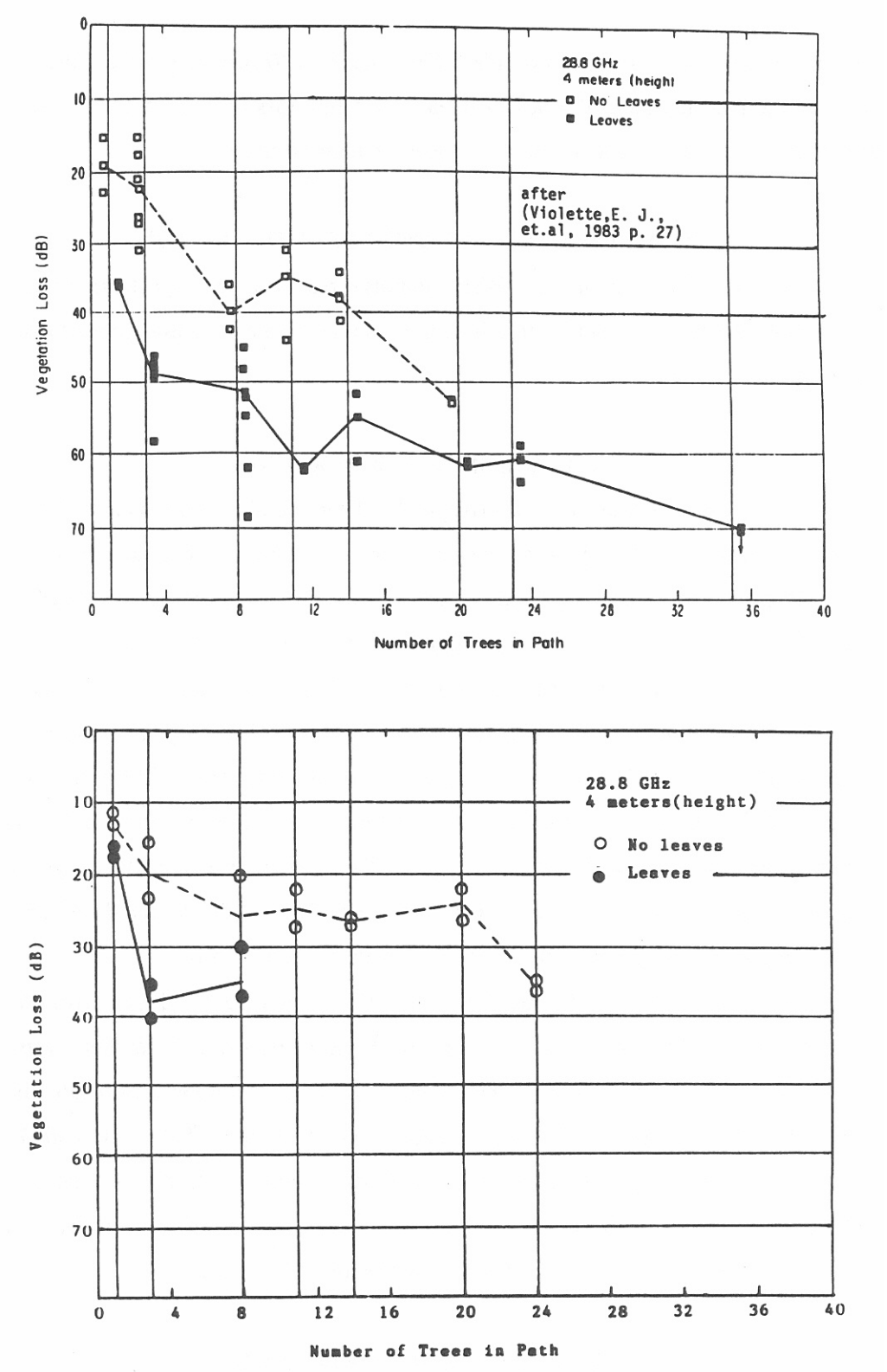

Figure 4.5. Vegetation loss as a function of the number of trees on path for 28.8 GHz at 4 meters.

in the 1982 measurements. Using an average foliage depth of 10 meters per tree, these results are not dissimilar from the 1982 measure of a nearly linear vegetation loss rate of 1.5 to 2.0 dB per meter out to 30 meters, with a much decreased rate at greater than 30 meters.

5. DATA ANALYSIS AND RESULTS (30.3 GHz)

The four data types (amplitude, BER, impulse response and spectrum scans) measured at 30.3 GHz were discussed in Section 3. In this section, some of each of these types of data are presented for comparison and analysis.

5.1 Amplitude Data at 30.3 GHz

The data in Figures B.1 through B.8 (Appendix B) are similar to the data in Figures A.1 through A.8, respectively, except for the operating frequency and the manner of data acquisition. These figures are listed in Table 5.1. The paths and locations for the two sets of figures are identical.

The measurements for Figures A.1 through A.4 (28.8 GHz) and B.1 through B.4 (30.3 GHz) were made with no leaves on the trees and the measurements for Figures A.5 through A.8 (28.8 GHz) and B.5 through B.8 (30.3 GHz) were made with leaves on the trees. The vegetation loss at 30.3 GHz is generally greater than at 28.8 GHz for both the foliated and defoliated state. The pattern broadening with trees on path at 30.3 GHz is similar to the 28.8 GHz data. For Path 1 in Figure B.5, B.6, B.7 and B.8 (measurements with leaves), the vegetation loss generally exceeded the dynamic range of the receiving system at 3 and 8 trees. However, for Path R in these same figures, the received signals were sufficient to be recorded and again demonstrate the difference in Path 1 and Path R.

The data in Figures 5.1 and 5.2 are the results of plotting peak amplitudes from the azimuth and elevation scans from Paths 1 and R at 1 meter and 4 meter transmitter heights, respectively, as in Figures 4.1 and 4.2 of the 28.8 GHz data, these figures show the differences in results due to leaves on the trees, and effects of the transmitter-receiver placement on the path (path 1 vs. Path R). There is at least a 10 dB increase in vegetation loss in the foliated state compared to the defoliated state and about 10 dB more vegetation loss on Path 1 (transmitter in the clear), when compared to Path R (transmitter in the trees). The data in Figure 5.3 is a composite of Figures 5.1 and 5.2

5.2 Bit-Error-Rate Data at 30.3 GHz

For each recording of received signal amplitude at 30.3 GHz, a corresponding bit-error-rate (BER) reading was recorded. Examples of the 30.3 GHz amplitude data and the corresponding BER data

Table 5.1. Amplitude Scan Data at 30.3 GHz

Figure Number	Scan Azimuth/Elevation	Transmitter Height (Meters)	Foliage State Leaves - No Leaves
B.1	Azimuth	1	No Leaves
B.2	Azimuth	4	No Leaves
B.3	Elevation	1	No Leaves
B.4	Elevation	4	No Leaves
B.5	Azimuth	1	With Leaves
B.6	Azimuth	4	With Leaves
B.7	Elevation	1	With Leaves
B.8	Elevation	4	With Leaves

were shown in Figure 3.6. The data in Figures C.1 through C.8 (Appendix C) are additional displays of the bit error rate measurement results. These displays are identical to Figures B.1 through B.8 in regard to scan angle, transmitter height, and path, and make signal amplitude/bit-error-rate pairs. These Figures are listed in Table 5.2.

Two factors affect the measured BER. The first is the received signal-to-noise ratio, such that, all other things being equal, a high signal-to-noise level results in a low BER. Comparing the calibration columns of Figures 8.1 and C.1, a strong correlation between the received signal level and the BER is evident. The second factor affecting BER is the presence of multipath signals, such as those observed in the impulse response records. The degree of degradation in BER performance due to multipath interference depends on the delay time and relative amplitude of the delayed signal to the direct signal. It is difficult to separate, in these data, instances of multipath dominance over the received signal-to-noise effect. This is true because 1) the sampled data were rounded to the nearest power of 10, and 2) the limited number of samples within a given system gain range do not provide a basis for the comparison.

A review of the data in Figures C.1 through C.4 (defoliated trees) shows that, in nearly all cases at 1 tree and 3 trees, one or more operating angles produce low BERs of 10E-8 within the scan range.

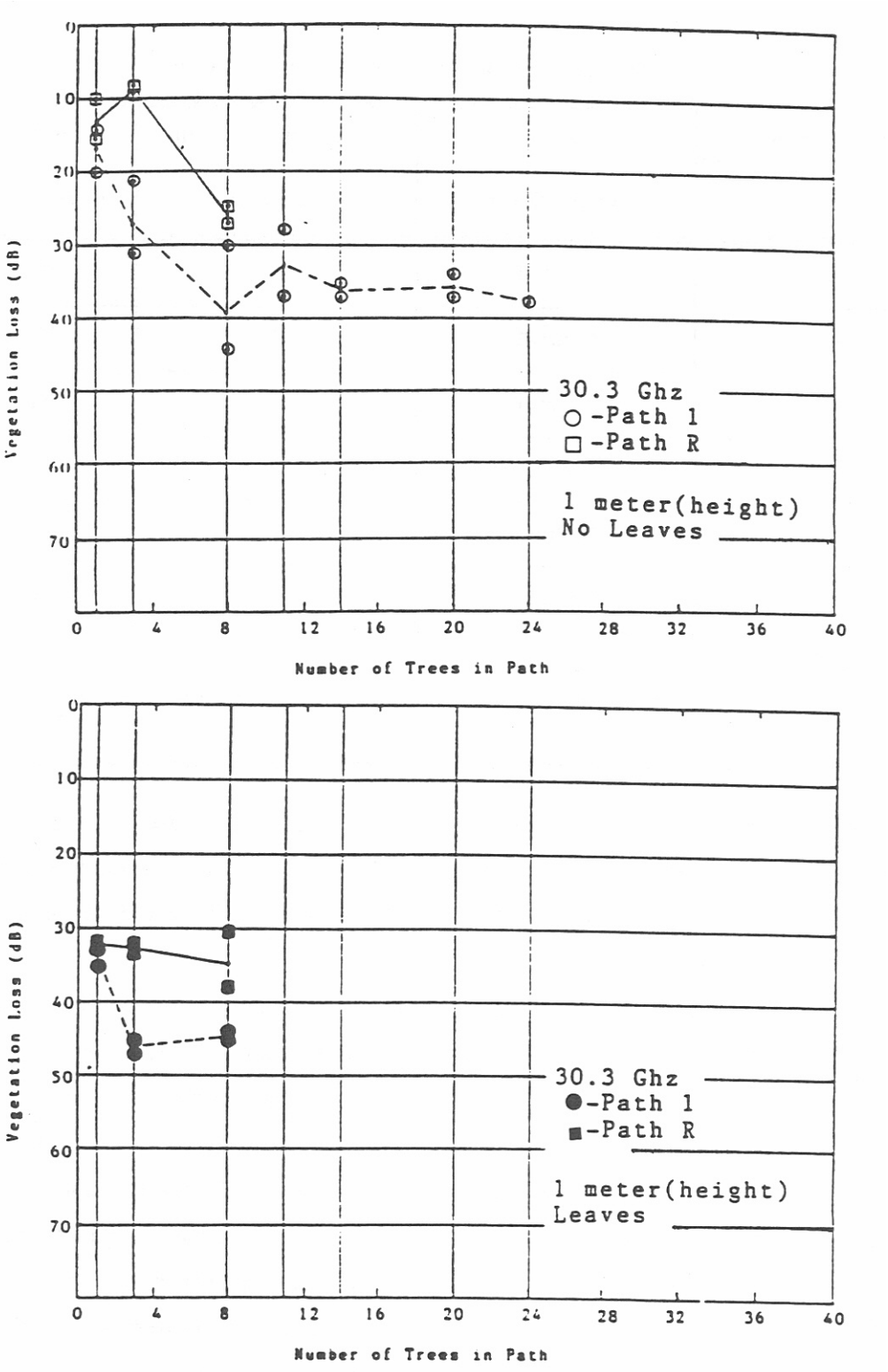

Figure 5.1. Vegetation loss values as a function of trees on path (the connecting lines indicate average values). Measurements at 1 meter transmitter height.

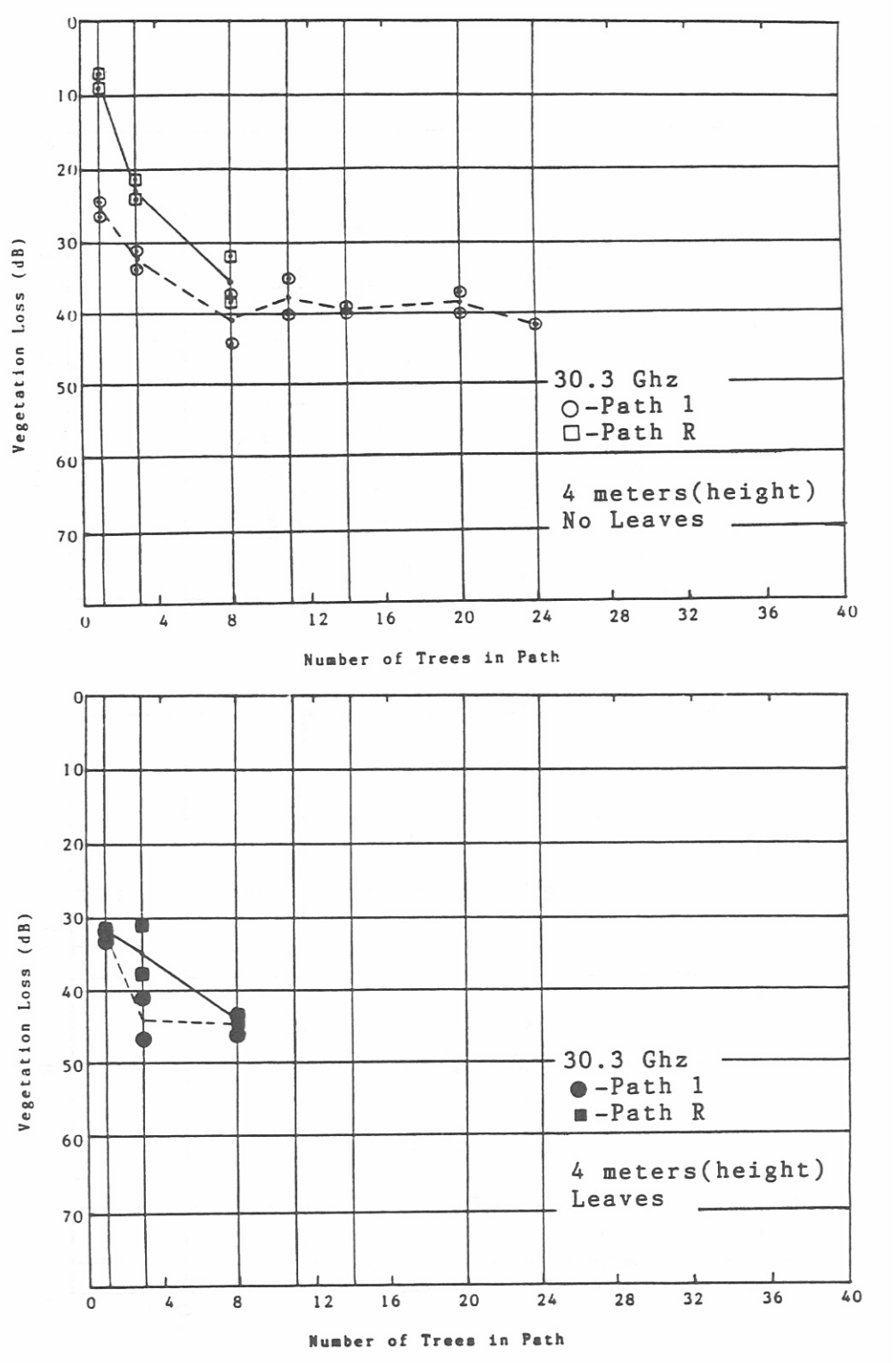

Figure 5.2. Vegetation loss values as a function of trees on path. (The connecting lines indicate average values). Measurements at 4 meter transmitter height.

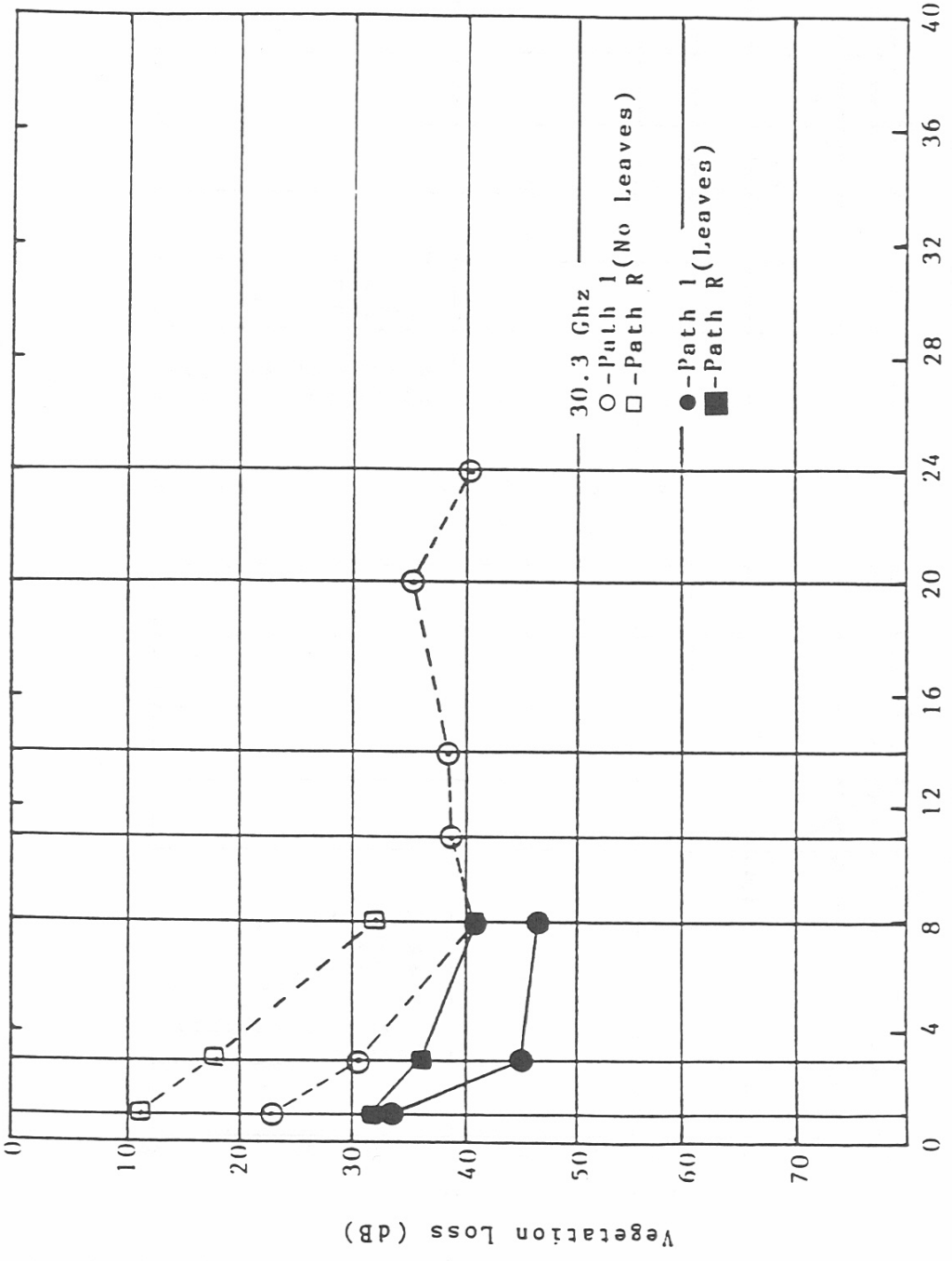

Figure 5.3. Vegetation loss values as a function of trees on path. These values are the average of the 1-meter and 4-meter transmitter height data.

TABLE 5.2 BER SCAN DATA AT 30.3 GHz

Figure Number	Scan Azimuth/Elevation	Transmitter Height (Meters)	Foliage State Leaves - No Leaves
C.1	Azimuth	1	No Leaves
C.2	Azimuth	4	No Leaves
C.3	Elevation	1	No Leaves
C.4	Elevation	4	No Leaves
C.5	Azimuth	I	With Leaves
C.6	Azimuth	4	With Leaves
C.7	Elevation	1	With Leaves
C.8	Elevation	4	With Leaves

In Figures C.5 through C.8 (foliated trees) many of the scans at 3 trees and 8 trees show no low BERs which corresponds to the high vegetation loss values in the same scans of Figures B.5 through B.8.

5.3 Impulse Response Data at 30.3 GHz

Unlike the continuous antenna scans recorded for the amplitude and BER, impulse response data was recorded at preset angles. These angles are also measured with respect to the transmitter-receiver line of site in the azimuthal (horizontal) plane, and in the elevation (verticle) plane. A set of impulse data recordings made at several azimuthal angles is called an azimuthal scan, and a set of elevation impulse data is called an elevation scan. Each data record displays signal arrivals out 20 ns after the direct arrival. The impulse response system is capable of recording delays out to a maximum of 254 ns. Examples of these individual records were shown in Figure 3.7 and discussed in Section 3. The impulse amplitude response is calculated from the recorded co- and quad-phase components.

As an aid for studying the overall results from a full scan, displays such as Figure 5.4 were composed for several of the data sets. Figure 5.4 is a three-dimension plot of the azimuth scan of the Path 2 calibration set with the transmitter at the 4 meter height.

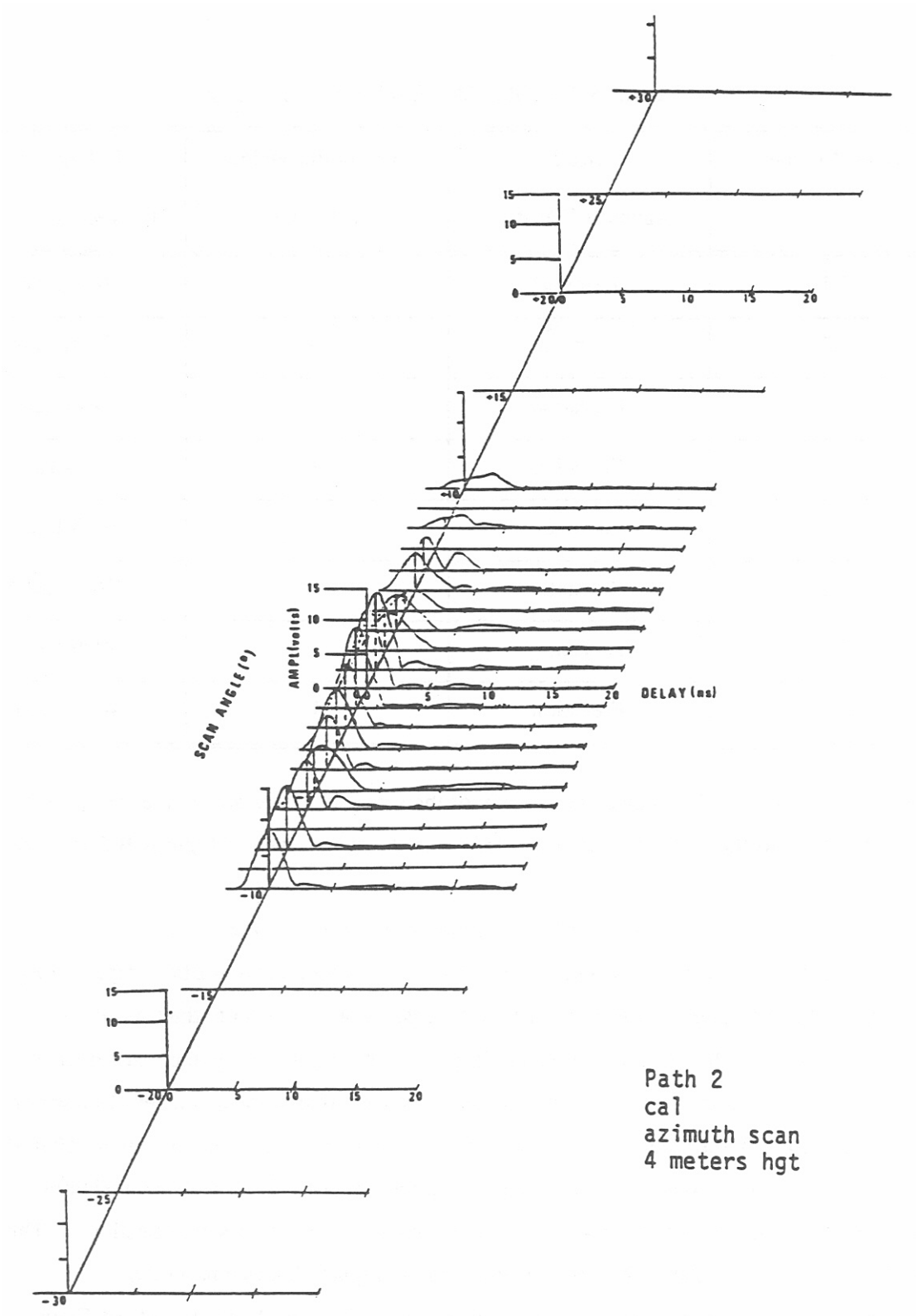

Figure 5.4. Impulse response records for the Path 2 azimuth calibration scan at 4 meter transmitter hight.

In these displays, each individual impulse is aligned such that the center of its direct component occurs at a zero time delay, and the impulse response amplitude is traced with the reference amplitudes of the response and display grid aligned. Within each impulse response record, the delayed components are relative in voltage amplitude to the zero delay reference and to each other. For each impulse response recorded at different azimuthal angles, the input attenuation was adjusted in 6 dB steps to receive a near maximum level from the AGC amplifier, without saturating it. Approximate amplitude levels at zero time delay for the display in Figure 5.4, could be determined from Path 2, 4 meter, azimuthal calibration display in Figure A.2. The impulse response plots (Appendix D) that were prepared for this section are listed in Table 5.3. Figures D.1 through D.20 are plots from measurements with no leaves present and Figure D.21 through D.30 are plots from measurements with leaves. The table shows comparative data (with and without leaves) from similar paths. Where there are no figures in the (with leaves) column, either there was no recorded data or the records in each plot were of insufficient quality to warrant inclusion in this report. In Figure 5.4, delay components of significant amplitude are present out to about 3 ns.

A set of six composites from Path 2 are shown in Figures D.1 through D.6., all from recordings at the 4 meter transmitter height. These include the azimuth calibration scan (Fig. 5.4) and elevation and azimuth scans with 1 tree, 3 trees, and 8 trees on the path. There is evidence of multipath signals in all of these data sets, but not necessarily at each scan angle. Figures D.1 and D.2 show plots of elevation and azimuth scans, respectively, for 1 tree on path. Here, longer delay values are observed, such as 5 ns at +20° azimuth. Figures D.3 and D.4 are plotted from the 3 tree data and show some delay values out to 15 ns. Delays of significant amplitude are observed in Figure D.4 (an azimuth scan) out to ±-30°. In the final set of Path 2 impulses, Figures D.5 and D.6, there are considerably delayed signals at the smaller scan angles (±-5°), with reduced direct signal amplitude beyond -10°. No data was available from +6° to +30° in Figure D.6.

Because no measurements were made beyond 8 trees on Path 2, and because some of the data were missing at 1 tree, 3 trees, and 8 trees on Path 1, the 11 tree and 14 tree measurements from Path 1 (shown in Figures D.7 through D.10) are used as an extension of Path 2 in this study. The impulse response data in Figures D.7 and D.8 are from the elevation and azimuth scans, respectively, for 11 trees. In Figure D.7 data are available between ±-6° only, because the received signal amplitude outside these angles was too small to trigger the impulse sampling circuit. Delay values are observed out to 10.ns in these displays. Figures D.9 and D.10 show the impulse response data from the elevation and azimuth scans, respectively, at 14 trees. In these plots, even more impulses are missing due to weak

TABLE 5.3 IMPULSE RESPONSE PLOTS

Figure No. (No Leaves)	Figure No. (Leaves)	Path	Scan	No. of Trees
D.1	D.21	2	Elevation	1
D.2	D.22	2	Azimuth	1
D.3	D.23	2	Elevation	3
D.4	D.24	2	Azimuth	3
D.5	D.25	2	Elevation	8
D.6	D.26	2	Azimuth	8
D.7		1	Elevation	11
D.8		1	Azimuth	11
D.9		1	Elevation	14
D.10		1	Azimuth	14
D.11	D.27	R	Elevation	1
D.12	D.28	R	Azimuth	1
D.13	D.29	R	Elevation	3
D.14	D.30	R	Azimuth	3
D.15		R	Elevation	8
D.16		R	Azimuth	8
D.17		D	Elevation	1.8
D.18		D	Azimuth	1.8
D.19		D	Elevation	3.3
D.20		D	Azimuth	3.3

received signal levels. Delay values in these plots are in the 3 to 5 ns range.

The impulse response data in Figures D.11 through D.16 are from the elevation and azimuth scans for 1 tree, 3 trees, and 8 trees on Path R. These data are from the same paths as the corresponding 1 tree, 3 tree, and 8 tree data taken on Path 1, except that the locations of the transmitter and receiver are reversed. As was the case with the 30.3 GHz amplitude data, the terminal reversal had the effect of reducing the amplitude broadening with scan angle, which in turn inhibited impulse response triggering

at the large scan angles. For this data set, the scan was limited to ±-20° azimuth. In this data set, the delayed signals are primarily within ±-10°, with maximum delay values of about 10 ns. Several of the impulse response plots contain multiple delay values.

The final set of impulse response data, in Figures D.17 through D.20, is from Path D. As observed in Figure 3.3, this path is diagonal to the row pattern of the orchard. The tree density values 1.8 and 3.3 are calculated by adding the fractional parts of all the trees which lie on the propagation path. The impulse response traces show delayed signals which lie primarily within ±-15° of the direct pointing angle, and several of these show multiple delay signals.

The remaining impulse response plots in Figure D.21 through D.30 were from measurements with leaves on the trees. Figures D.21 through D.26 (with leaves) correspond respectively to Figures D.1 through D.6 (without leaves), all recorded on Path 2. The delayed impulse components from these two sets of data have similar delay and amplitude characteristics, except that for 8 trees (with leaves) in Figures D.25 and D.26, the increased vegetation loss inhibited sufficient impulse trigger at the larger scan angles. In Figures D.27 through D.30, which were recorded on Path R (with leaves) and correspond to the no leaves data in Figures D.11 through D.14, the reduced signal level (increased vegetation loss) caused an even greater reduction of useful records at scans beyond ±-5°.

5.4 Frequency Spectra Data at 30.3 GHz

At selected receiver angle positions on each of the paths, the frequency spectrum of the received wideband IF signal was recorded. The selection, which totaled 70 individual spectrum plots from the "no leaves" measurements, and 42 from the "leaves" measurements, spanned all paths. Examples of these spectra were shown in Figure 3.8 along with the corresponding impulse response data for the same scan position. The data in Figure 3.8 are reprinted in Figure 5.5 to illustrate the relationship between the IF frequency spectrum and the corresponding impulse response. Both data types indicate multipath signals when they are present. In the impulse response, the relative amplitude and the delay time of multipath signals can be read directly from the time scale. In the frequency spectra plots, the nulls in the frequency domain caused by the multipath signal interfering with the direct signal can be seen. The spacing of these nulls is proportional to the inverse of the delay time of the multipath signal which produces them. For example, a 1 ns delay results in a null spacing of 1 GHz, a 10 ns delay results in a null spacing of 0.1 GHz, etc. In Figure 5.5 (a), the spectrum is smooth, indicating the absence of any received multipath signals. The corresponding impulse response in Figure 5.5 (b) indicates that no multipath signals are present as well. The data in Figures 5.5 (c) and (d) show the presence of strong multipath signals. The

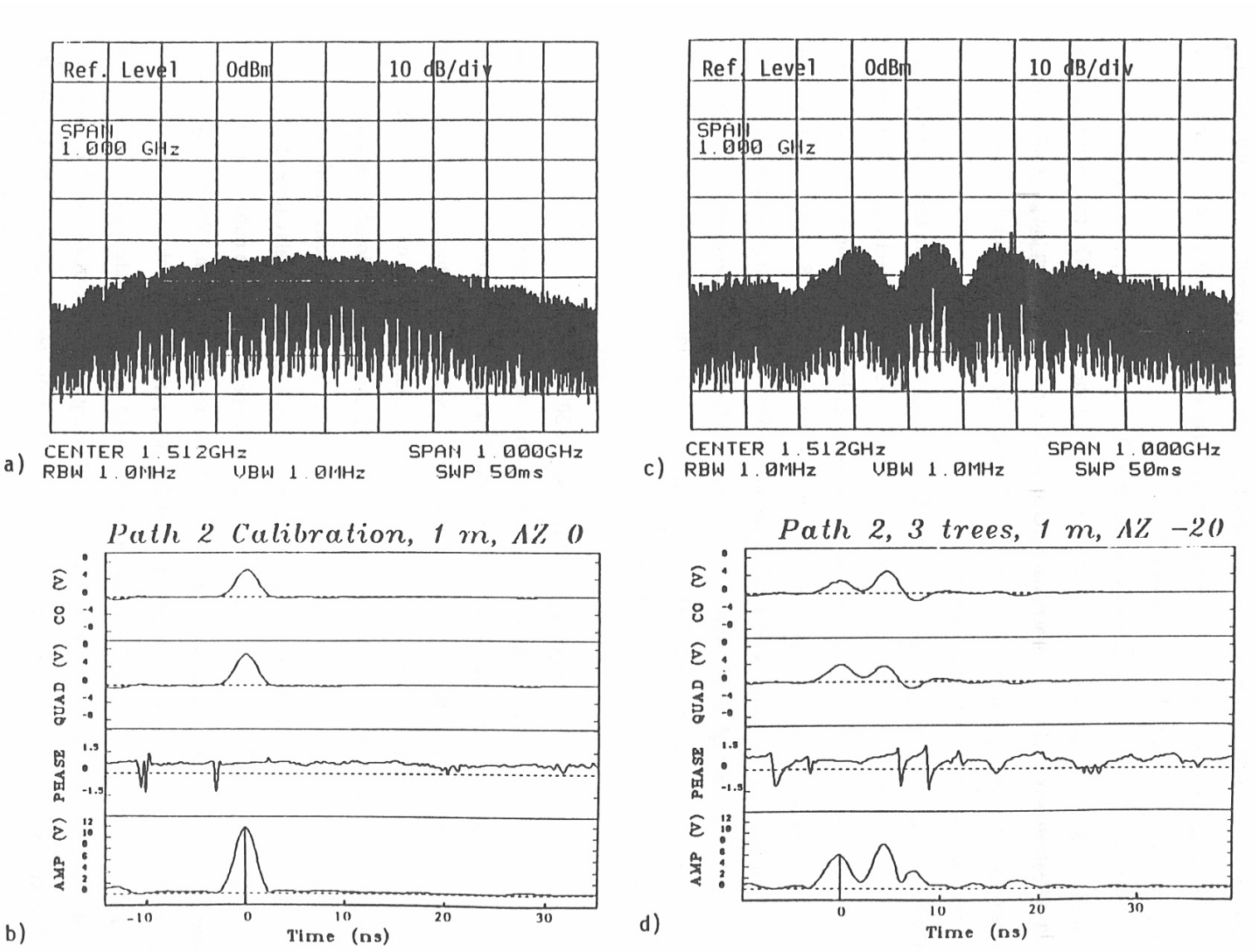

Figure 5.5. Frequency spectra and corresponding impulse response data for calibration and 3 trees on Path 2.

spectrum in Figure 5.5 (c) has null spacings from 0.15 to 0.20 GHz, which indicate time delays of about 5 to 7 ns. The impulse response in 5.5 (d) show multipath signals at 4.5 and 7.0 ns. These data compare well. In a situation with only one multipath signal present, and with a delay time of 4 ns or greater, the null pattern on the spectrum plot and the multipath component in the impulse response could both be easily read and compared. However, this seldom will be the case in these measurements. Additional data sets are shown in Figures 5.6 and 5.7. The impulse response/spectrum pair in Figure 5.6(c) and (d) show nulls at .4 GHz, which corresponds to a delay component at 2.5 ns. The slightly distorted backside of the direct signal impulse in Figure 5.6 (d) would support the presence of a multipath component in that delay range. The presence of the several multipath components in the remaining sets in Figure 5.6 and Figure 5.7, are more difficult to compare. None of the foliated spectra are included because they are very similar to the defoliated results.

6. CONCLUSIONS

Measurements at 30.3 GHz, using a wideband probe provided a characterization of the effects of vegetation on the propagation of millimeter-wave signals. The wideband measurements included vegetation loss, impulse response records to measure multipath, and a measure of the received signal BER. Additional measurements were made at 28.8 GHz to describe vegetation loss. A pecan orchard near Wichita Falls, Texas, (used for earlier measurements) was used for the test site because of the uniformly planted trees. Measurements were made at 1 and 4 meter heights with no leaves and again with leaves.

The received signals at 28.8 and 30.3 GHz when normalized for path length differences produced a measure of vegetation loss due to trees on the propagation path. A vegetation loss rate of 1.5 to 2.0 dB per meter as a function of foliage density (similar to the 1982 measurements) was observed for the first 30 meters (3 tree depth), and a much reduced rate was observed beyond 30 meters. An approximate 10 dB greater vegetation loss was observed with leaves on the trees compared to no leaves.

A marked difference occurred in the illumination of the trees on the path as the result of interchanging the positions of the transmitter (widebeam antennas) and the receiver (narrow beam antennas). When a major segment of the path was open field with the transmitter in the open field and the receiver in the orchard at a close proximity to the first tree on path, a nearly uniform signal intensity was measured across a ± 30° azimuth scan at 8 trees (80-meter foliage density). In the reverse mode (receiver in the open field and transmitter in the orchard), much more antenna directivity was observed

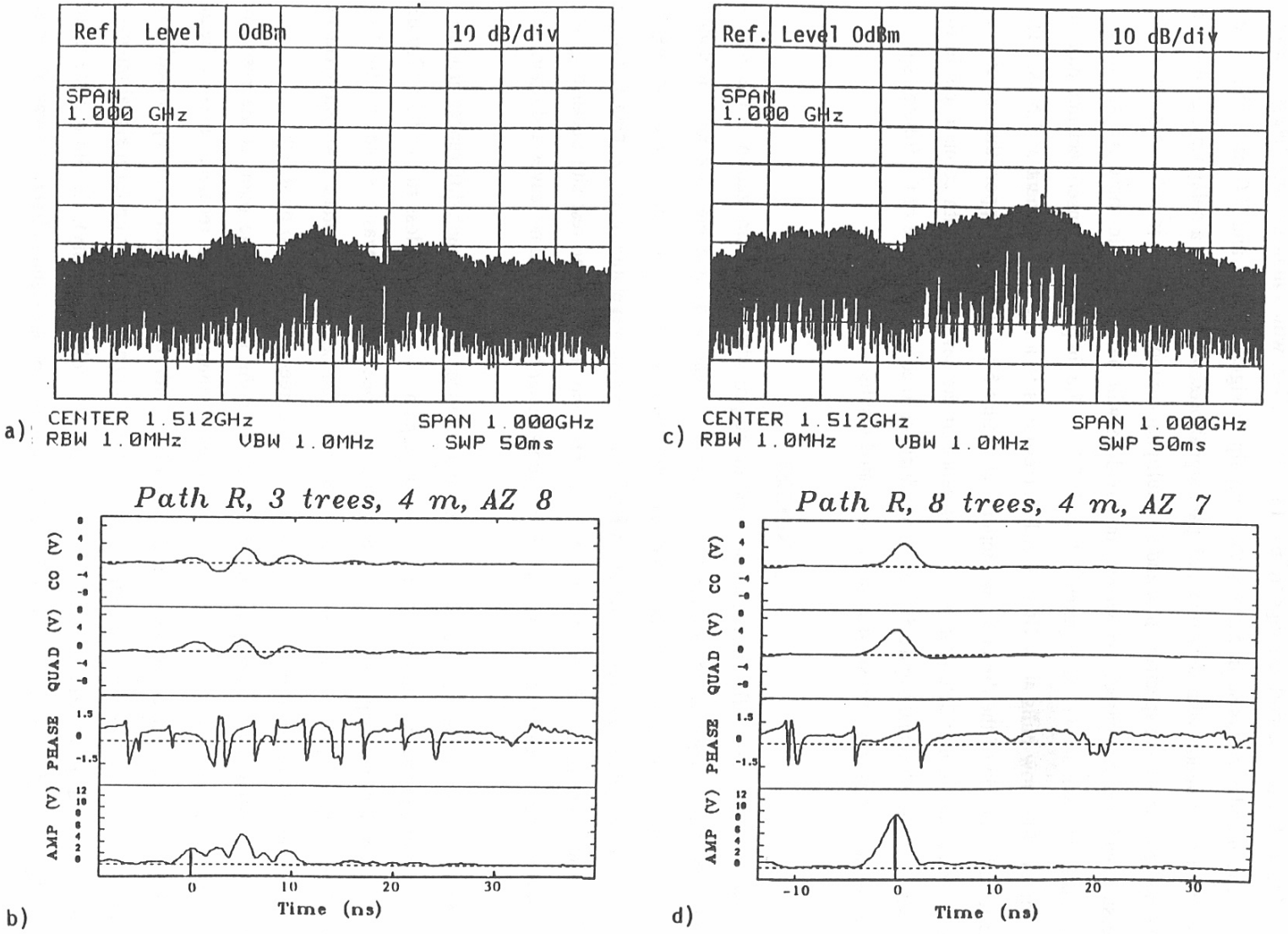

Figure 5.6. Frequency spectra and corresponding impulse response data for 3 trees and 8 trees on Path R.

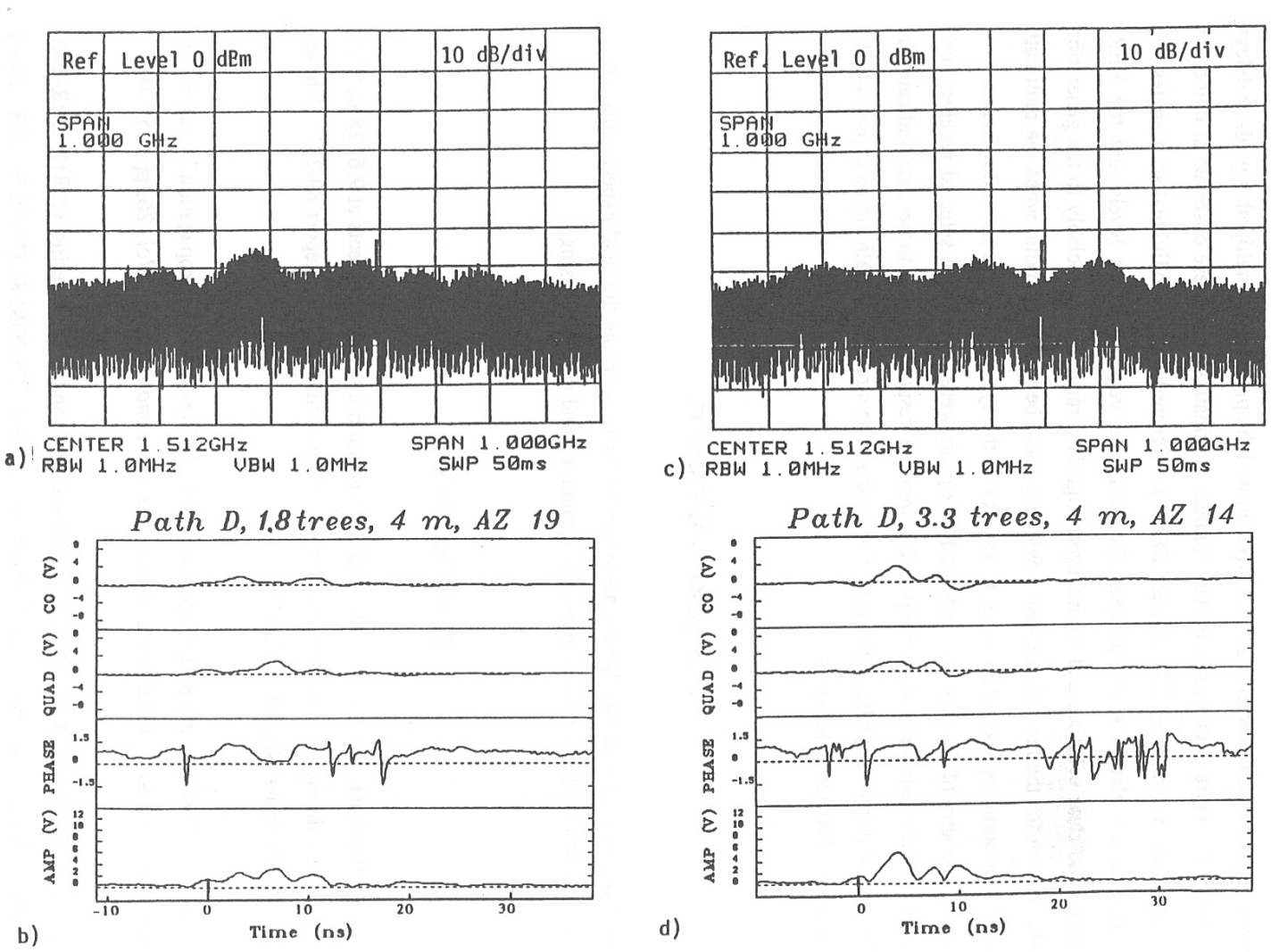

Figure 5.7. Frequency spectra and corresponding impulse response data for 1.8 trees and 3.3 trees on Path D.

with an approximate 10 dB average increase in the peak received signal level.

Impulse response measurements at 30.3 GHz showed the presence of multipath signals at delays out to 15 ns. From the more than 30 sets of data studied, multipath signals were observed at numerous scan angles out to the maximum ± 30°. System BERs were recorded at all individual scan angles. A very strong inverse correlation exists between the measured vegetation loss levels and the BER. However, there is no clear evidence that the multipath signals contributed appreciably to the generation of errors. One reason for the lack of conclusive evidence could be that at the point when the multipath and direct signals became approximately equal in amplitude, the system signal-to-noise dominates.

Frequency spectra of the received wideband IF signals were recorded at selected receiver scan angle positions. When compared to corresponding impulse response plots, these data indicate the presence of similar multipath signals. However, if more than one strong multipath signal is present, the spectra data become difficult to interpret.

7. ACKNOWLEDGMENTS

The authors wish to acknowledge the assistance by Yeh Lo during the field experiments, and Robert DeBolt and Glenn Salaman for computer programming and data processing.

8. REFERENCES

Jones, D.L., R.H. Espeland, and E.J. Violette (1989), Vegetation loss measurements at 9.6, 28.8, 57.6, and 96.1 GHz through a conifer orchard in Washington State, NTIA Report 89-251, October, 69 pp., (NTIS Order No. PB 90-168717).

Schwering, F.K., E.J. Violette, and R.H. Espeland (1988), Millimeter-wave propagation in vegetation: experiments and theory, *IEEE Trans. Geoscience and remote sensing*, Vol. 26, pp. 355-380.

Violette, E.J., R.H. Espeland, A.R. Mitz, F.A. Goodknight, and F. Schwering (1981), SHR-ENF propagation through vegetation on Colorado east slope, CECOM-81-CS020-F, U.S. Army Communications-Electronics Command, Ft. Monmouth, NJ, 07703.

Violette, E.J., R.H. Espeland, K.C. Allen, and F. Schwering (1983), Urban millimeter-wave propagation studies, Research and Development Technical Report CECOM-83-3, U.S. Army Communications-Electronics Command, Ft. Monmouth, NJ, 07703.

Violette, E.J., R.H. Espeland, and K.C. Allen (1983), A diagnostic probe to investigate propagation at millimeter-wave lengths, NTIA Report 83-128, August, 38 pp., (NTIS Order No. PB 84-104223).